

UC San Diego

UC San Diego Electronic Theses and Dissertations

Title

Negative Correlation between SMARCAD1 and Histone Citrulline Protein Expression in Cancer and Non-cancerous Cell Lines

Permalink

<https://escholarship.org/uc/item/5078x69h>

Author

Zhao, Tianyi

Publication Date

2016

Peer reviewed|Thesis/dissertation

UNIVERSITY OF CALIFORNIA, SAN DIEGO

Negative Correlation between SMARCAD1 and Histone Citrulline Protein
Expression in Normal and Cancer Cell Lines

A Thesis submitted in partial satisfaction of the requirements of the degree
Master of Science

in

Bioengineering

by

Tianyi Zhao

Committee in charge:

Professor Sheng Zhong, Chair
Professor Prashant Gulab Ram Mali
Professor Yingxiao Wang

2016

Copyright

Tianyi Zhao, 2016

All rights reserved.

The Thesis of Tianyi Zhao is approved and it is acceptable in quality and form for publication on microfilm and electronically:

Chair

University of California, San Diego

2016

Table of Contents

Signature Page.....	iii
Table of Contents	iv
List of Figures	v
List of Tables	vii
List of Graph	viii
Abstract of the Thesis.....	ix
Introduction.....	1
Results	4
Material and Methods	31
Discussion	38
Conclusion.....	41
References	42

List of Figures

Figure 1: Histone 3 Citrullination catalyzed by PADI	3
Figure 2: SMARCAD1 knockdown mouse ES cells (KD).....	4
Figure 3: Protein analysis of SMARCAD1 and GAPDH in mouse ES WT and KD cells	5
Figure 4: Protein analysis of Histone3, H3R26Cit, and His3R2/8/17Cit in mouse ES WT and KD cells	6
Figure 5: Protein analysis of PADI4 in mouse ES WT, KD and Cl+ cells, and potential relationship between SMARCAD1, PADI4 and Histone3 citrullination ...	9
Figure 6: Protein analysis of SMARCAD1, GAPDH, PADI4, and His3R2/8/17 in human non-cancer kidney cells and human kidney cell lines	11
Figure 7: SMARCAD1 CRISPR/Cas9 KO Plasmid.....	13
Figure 8: SMARCAD1 CRISPR/Cas9 HDR Plasmid	14
Figure 9: CRISPR/Cas9 KO/HDR co-transfection of HEK-297T kidney cells	15
Figure 10: SMARCAD1 primer set targeting HDR recombinase region.....	17
Figure 11: RNA and Protein Analysis of HEK-293T and HEK-293T KO Cells on SMARCAD1 expression level.....	18
Figure 12: CRISPR/Cas9 KO/HDR co-transfection of 786-0 kidney cancer cell line.....	20
Figure 13: Timeline of CRISPR/Cas9 KO/HDR co-transfection of A-498 and ACHN kidney cancer cell lines.....	21

Figure 14: CRISPR/Cas9 KO/HDR co-transfection of A-498 kidney cancer cells	23
Figure 15: CRISPR/Cas9 KO/HDR co-transfection of ACHN kidney cancer cells	24
Figure 16: Standard cell maintenance of A-498 and ACHN KO cells after CRISPR/Cas9 KO co-transfection	25
Figure 17: RNA and Protein Analysis of A-498, A-498 KO, ACHN and ACHN KO cells on SMARCAD1 expression level	26
Figure 18: Protein analysis of His3R2/8/17Cit and PADI4 in HEK-293T, HEK- 293T KO and HEK-293T Cl+ cells, and potential relationship between SMARCAD1, PADI4 and Histone3 citrullination	29
Figure 19: Protein analysis of His3R2/8/17Cit in A-498 and ACHN WT and KO cells	30

List of Tables

Table 1: Protein Samples Concentration and Western Blot Loading Condition ..	32
Table 2: Primary and Secondary Antibody Dilution Condition for Western Blot on Mouse ES Cells and SMARCAD1 KD #2 Cells	33
Table 3: Total RNA Concentrations	36
Table 4: RT-PCR Primer Sequence.....	36
Table 5: One-step RT-PCR Cycling Conditions.....	36
Table 6: RNA Gel Electrophoresis Loading Conditions	36
Table 7: qRT-PCR RT Conditions	36
Table 7: qRT-PCR RT Conditions, Continued	37
Table 8: qRT-PCR cDNA Concentration	37
Table 9: qRT-PCR Cycling Conditions	37
Table 10: qRT-PCR Results	37

List of Graph

Graph 1: qRT-PCR results of SMARCAD1 and GAPDH RNA fold change in WT and KO HEK-293T, A-498 and ACHN cell lines	27
---	----

ABSTRACT OF THE THESIS

Negative Correlation between SMARCAD1 and Histone Citrulline Protein
Expression in Normal and Cancer Cell Lines

by

Tianyi Zhao

Master of Science in Bioengineering

University of California, San Diego, 2016

Professor Sheng Zhong, Chair

SMARCAD1 is a matrix-associated actin-dependent regulator of chromatin that encodes SWI/SNF subfamily of helicase proteins. It has been shown that the functions of SMARCAD1 are linked to histone 3 citrullination, a specific type of histone post-translational modifications. Histone citrullination can lead to alterations in protein functions, and affect gene expressions. This peptidylarginine deiminases (PADIs) catalyzed post-translational modification also increases in the

progression of cancer. Interestingly, human renal cancer cells exhibit low to non-detection of SMARCAD1 protein expression. It is anticipated that an association between SMARCAD1 and histone 3 citrullination function critically in renal cancer and tumor formation. Western blot was performed on mouse cells first followed by multiple renal cancer and non-cancer human cell lines, to determine SMARCAD1 and histone 3 citrullination protein expression levels and their potential correlation. Multiple cell treatments were introduced and CRISPR/Cas9 gene editing system was used to create SMARCAD1 gene knocking out condition. A negative correlation was determined between SMARCAD1 and citrullination expression level, with a potential positive feedback loop in between SMARCAD1 and histone 3 citrulline enzyme PADI4 in certain cell lines. Moreover, this negative correlation between two protein levels serves as an indicator of renal cancer existence; decrement of SMARCAD1 protein level holds true in renal cancer cells, in parallel with an increment of the histone 3 citrulline protein expression.

Introduction

SMARCAD1 is a SWI/SNF-related, and matrix-associated actin-dependent regulator of chromatin. SMARCAD1 is located on chromosome 4, specifically from position 94207608 to 94291292, and it is a member of the DEAD/H box-containing helicase superfamily, which include proteins essential to genome replication, repair, and expression [1]. Recent study shows that this SWI/SNF-like protein is a key factor required in restoring and maintaining silenced heterochromatin domains [2]. Heterochromatins are condensed regions of the chromatin and play an important role in gene expression. Heterochromatin instability has the potential to generate very diverse gene expression profiles, and in cancer, the tightly normal packaging of heterochromatin is often compromised [3]. Thus, it is crucial to have a proper regulator of the heterochromatic regions to potentially prevent tumor formation. Yet, the functions and roles that SMARCAD1 plays during cancer development remain unclear.

One evidence shows that SMARCAD1 function can be linked to histone modifications, and changes in histone modifications in heterochromatin correlate with the localization of SMARCAD1 protein [2]. Our lab's previous research has shown a strong co-localization of SMARCAD1 to histone post-translational modifications, especially histone 3 citrullination. Histone citrullination, also called deimination, is the post-translational conversion of an arginine to the non-coded amino acid citrulline and enzymes called peptidylarginine deiminases (PADIs) [4] perform this process. Accordingly, citrullination increases the hydrophobicity of a protein, leading to alterations in protein folding and functions [5]; this process can

also lead to decondensed chromatin [6] (Figure 1). In recent years, researchers have found that citrullination by PADIs of transcription factors, co-regulators, and histones affects gene expression in multiple tumor cell lines [6]. This modification can occur in pathological condition such that an increased level of citrullination is presented in the progression of cancer [7]. Moreover, the functional importance of histone 3 citrullination is thought to be directly related to gene regulation in cancer [8].

Still, there has been no single study showing how SMARCAD1 contributes to cancer formation. Interestingly, one research conducted by the Human Protein Atlas shows that in normal kidney cells, there is a high level of antibody staining for SMARCAD1 protein expression. However in renal (kidney) cancer tissues, protein expression level for 3 out of 12 samples have medium SMARCAD1 level; while 2 out of 12 have low level, and surprisingly the rest 7 samples all showed no protein detection [9].

Based on all the published findings on the functions of SMARCAD1, and histone citrullination, and how they all affect heterochromatin regulation, it is possible to hypothesis that there is a specific type of correlation between SMARCAD1 and PADI catalyzed citrullination, specifically histone 3 citrullination; together they have critical functions in multiple normal and cancer cell lines. Furthermore, SMARCAD1 can act as an indicator of the presence of kidney cancer.

To test this hypothesis, SMARCAD1 protein expression level was first tested in parallel with histone 3 citrulline and PADI protein level in mouse ES cells under several conditions (SMARCAD1 knockdown and PADI inhibition), to see if

there is any patterned correlation. Similar experiments were then carried out in human kidney cancer and non-cancer cell lines to test if the observed pattern in mouse cell line could potentially be established in human cell lines as well, and if this patterned correlation between SMARCAD1 and histone 3 citrulline protein level actually relates to human kidney cancer. The novel technique CRISPR/Cas9 gene editing system was also employed to knock out the entire SMARCAD1 gene in human kidney cell lines, in order to examine the hypothesis under different cell conditions.

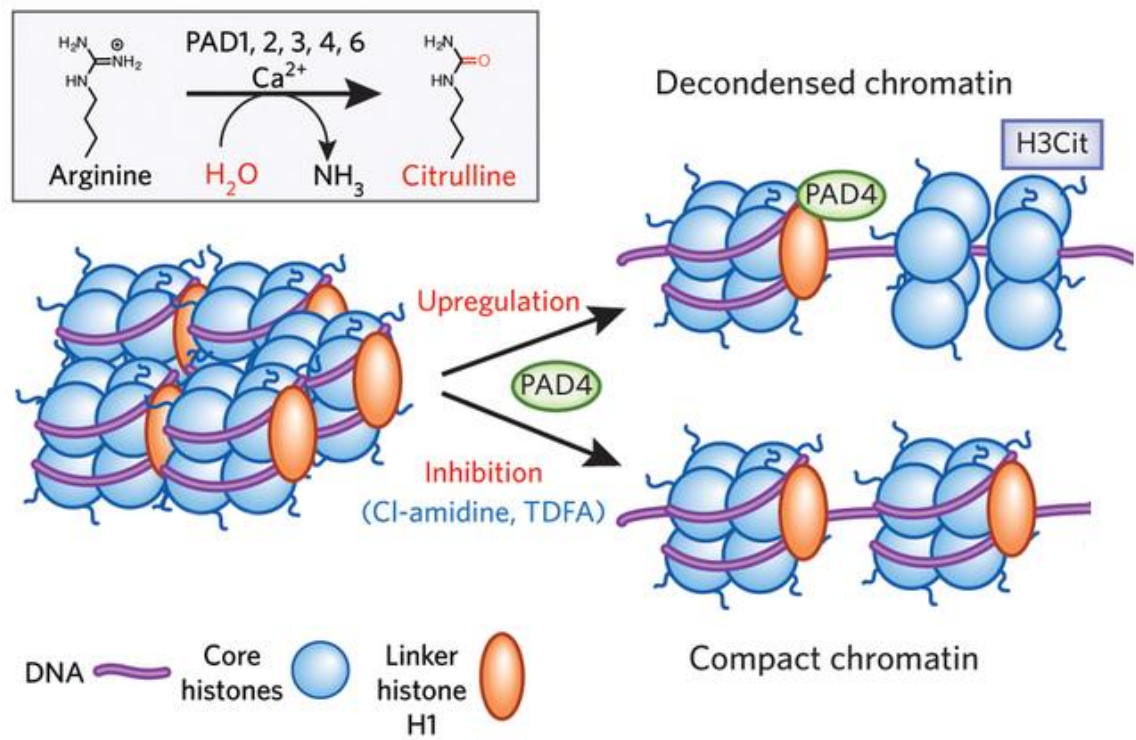


Figure 1: Histone 3 Citrullination catalyzed by PADI. PADI converts arginine to citrulline in histones. PAD4 citrullinates core (H3 and H4) and linker (H1) histones, leading to chromatin decondensation. CI-amidine inhibits PAD4 and bring chromatin back to its compact form [10].

Results

Confirmation of SMARCAD1 knockdown in mouse embryonic stem cell (ES)

To confirm the successful knocking down of SMARCAD1 gene with shRNA in mouse ES cells, the cell morphology was examined under microscope followed by analyzing of SMARCAD1 protein expression level via western blot on both mouse ES cells (WT) and SMARCAD1 knockdown cells (KD) to test the knock down efficiency. The mouse WT cells showed a typical morphology of dome-shaped colonies (Figure 2A). Within 24 hours of shRNA transfection, WT cells started to stretch out along the membranes (Figure 2B). 48 hours after the transfection, a flatter shape was observed for the WT cell colonies (Figure 2C). Finally after 72 hours of the transfection, right before the protein extraction, transfected colonies obtained a flattened shape instead of the typical rounded shaped (Figure 2D).

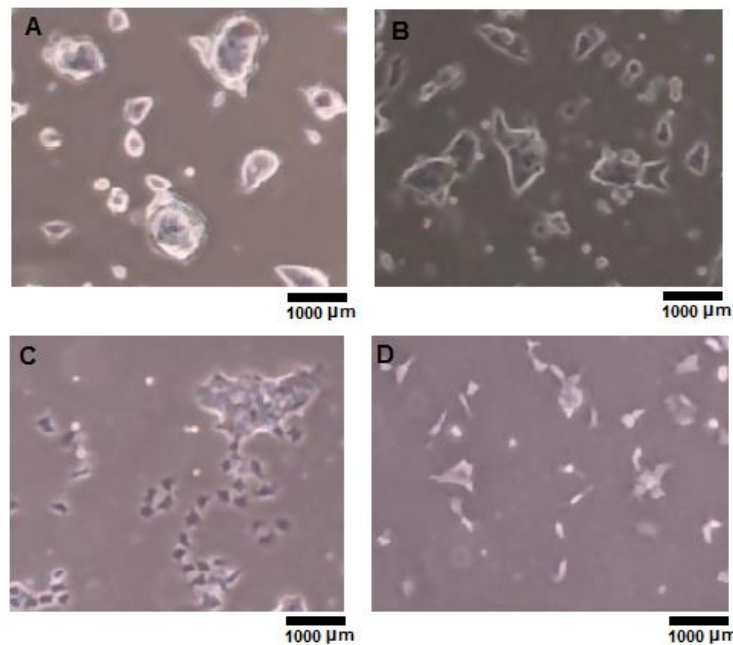


Figure 2: SMARCAD1 knockdown mouse ES cells (KD). Morphologies of the (A) wildtype mouse ES cells (WT) and SMARCAD1 shRNA knockdown cells KD after (B) 24 hours, (C) 48 hours, and (D) 72 hours of transfection.

GAPDH was used as an inner control to confirm the knocking down of the only target, SMARCAD1. Ponceau S staining of the membrane indicated a constant loading amount for both protein samples in all three groups (Figure 3A). The X-ray film showed a same protein expression level of GAPDH for all three sets of samples (Figure 3B), meaning that there is no modification on this housekeeping gene in between the two cell lines. SMARCAD1 protein level was significantly higher in mouse WT cells than in the KD cell line (Figure 3B). This data indicated a successful knocking down of the SMARCAD1 gene in the mouse WT cells while keeping a normal expression level of the other genes.

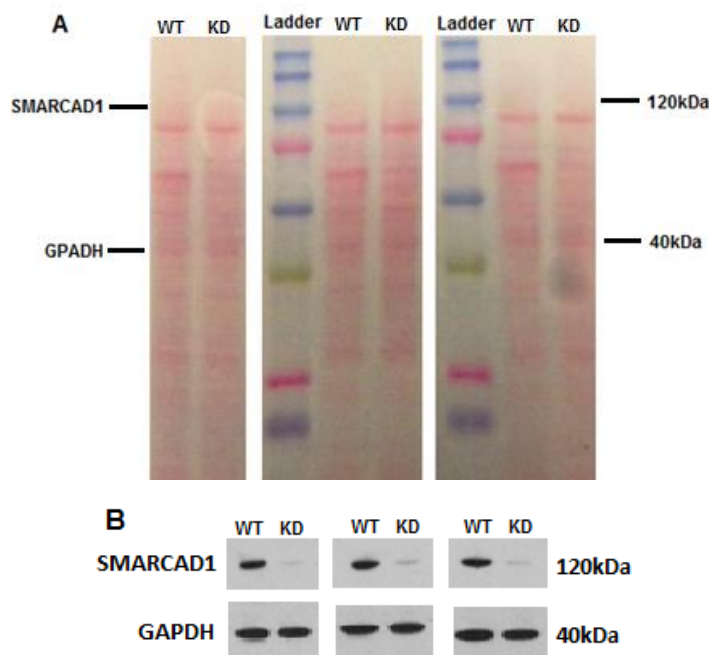


Figure 3: Protein analysis of SMARCAD1 and GAPDH in mouse ES WT and KD cells. (A) Ponceau S staining of the western blot membrane after transferring shows consistent protein loading amount for all protein samples. (B) Three repeats of SMARCAD1 and GAPDH expression level in the same amount of WT and KD protein samples. SMARCAD1 was anticipated at 117kDa, and the actually detection was around 120kDa. GAPDH was anticipated at around 37 kDa and detected at 40 kDa.

Repression of SMARCAD1 protein expression changes histone 3 citrullination level

To test the hypothesis that SMARCAD1 modulates histone 3 post-translational modification, specifically histone 3 citrullination, histone 3 (H3), histone 3 citrulline R26 (H3R26Cit), and Histone3 citrulline R2+R8+R17 (H3R2/8/17Cit) expression level were analyzed in both WT and KD protein samples.

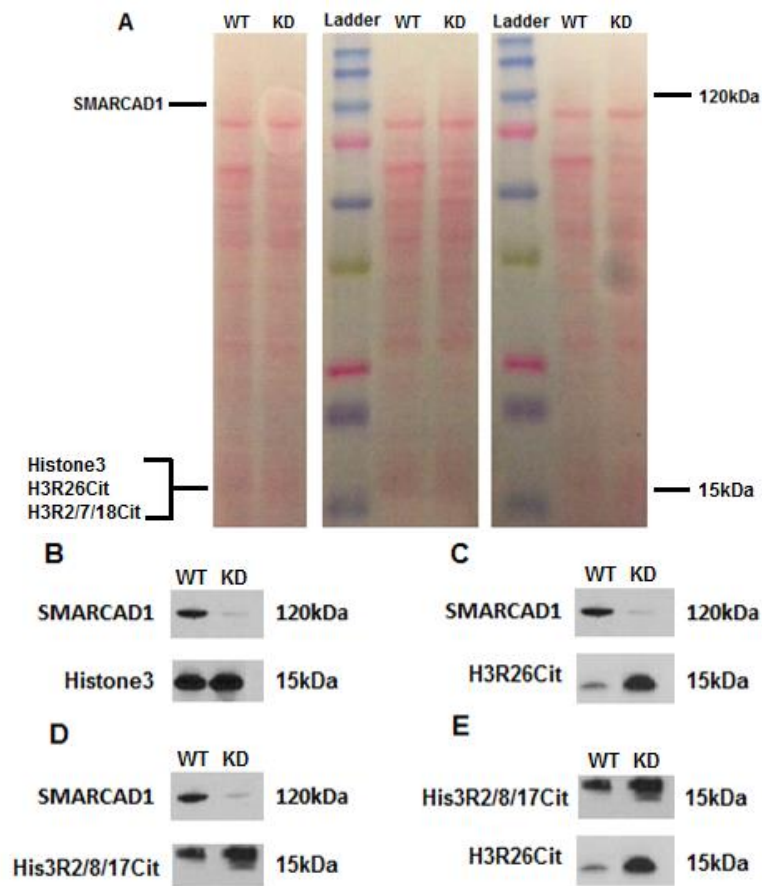


Figure 4: Protein analysis of Histone3, H3R26Cit, and His3R2/8/17Cit in mouse ES WT and KD cells. (A) Ponceau S staining of the western blot membrane after transferring shows consistent protein loading amount for all protein samples. (B) Histone 3 expression level in WT and KD. Histone 3 was detected at 15 kDa. (C) H3R26Cit expression level in WT and KD. H3R26Cit was detected at 15 kDa. (D) His3R2/8/17Cit expression level in WT and KD. Again, His3R2/8/17Cit was detected at 15 kDa. (E) Comparison between His3R2/8/17Cit and H3R26Cit expression level in WT and KD.

Ponceau S membrane staining result of the repeating samples showed a consistent amount of WT and KD protein samples (Figure 4A). The X-ray result showed that histone 3 level remained the same in both cells lines (Figure 4B); therefore, there was no change in histone 3 with a repression of SMARCAD1 gene. On the other hand, for the SMARCAD1 KD sample, both histone 3 citrullination marker H3R26Cit and H3R2/7/18Cit showed higher protein expression level (Figure 4C, Figure 4D). H3R26Cit expression level showed an even stronger negative correlation with SMARCAD1 gene repression comparing to H3R2/8/17 (Figure 4E). These results are in line with the hypothesis that repression of the SMARCAD1 gene in a normal functioning cell line increases the protein expression level of histone 3 citrullination, so there exists a negative correlation between SMARCAD1 and histone 3 citrullination, at least in the protein level.

Existence of a potential positive feedback loop between SMARCAD1 and protein arginine deiminase (PADI4)

In order to see whether SMARCAD1 has any correlation with the upstream mechanism that causes histone 3 citrullination, both WT and KD samples were tested for the expression level of protein-arginine deiminase (PADI), an enzyme that catalyzes the post-translational modification of arginine residues on histones to form citrulline. When tested for SMARCAD1 and PADI4 in WT and KD samples, a potential positive feedback loop was first observed (Figure 5C). With a lower SMARCAD1 protein expression level, KD sample actually showed a lower protein level of PADI4 comparing to WT (Figure 5A). To see if PADI4 modification will in turn modulate SMARCAD1, WT cells were treated with Cl-amidine (Cl+), a known

inhibitor of PADI4 deimination activity [4] and can bring chromatin back to its compact form (Figure 1). Protein analysis was then performed on CI+ and WT samples. Surprisingly, with a significant knocking down of PADI4 gene in the CI+ sample as shown by its protein expression level (Figure 5B), SMARCAD1 protein level dropped as well (Figure 5B). Thus, it is clear that there is a positive feedback loop between SMARCAD1 and PADI4 in the protein level. A decrement in either SMARCAD1 or PADI4 protein expression level will lead to a decrement in one another.

Second, a negative correlation was observed between the SMARCAD1/PADI4 positive feedback loop and histone 3 citrullination. KD sample showed higher expression level of His3R2/8/17Cit comparing to WT (Figure 5A), which indicated the negative correlation between SMARCAD1 and histone 3 citrullination. CI+ sample with a lower PADI4 protein level also showed a slightly stronger His3R2/8/17Cit protein expression (Figure 5B), thus a negative correlation. This actually confirm the network shown in Figure 5C. Again, GAPDH and histone 3 levels were consistent throughout all samples (Figure 5A, Figure 5B). However, literatures indicate a positive correlation between PADI4 and Histone3 citrullination (Figure 5C). Still, the network shown here is reasonable. The lab previous indicated a strong binding of SMARCAD1 to the Histone3 citrullination dense regions in ES cells. This binding can inhibit the protein expression level of Histone3 citrullination, thus causing a negative correlation between SMARCAD1 and His3R2/8/17Cit. In addition, literatures state that PADI4 could catalyzed the formation of citrulline on histones, but due to the binding of SMARCAD1 onto the

histone 3 citrullination site, it may make it difficult for PADI4 to catalyze citrulline formation without bypassing SMARCAD1. Because the final target of the potential positive feedback loop between SMARCAD1 and PADI4 is always histone 3 citrulline, and there is a negative correlation between SMARCAD1 and histone 3 citrullination, a decrement in PADI4 protein level could potential increase His3R2/8/17Cit protein expression level.

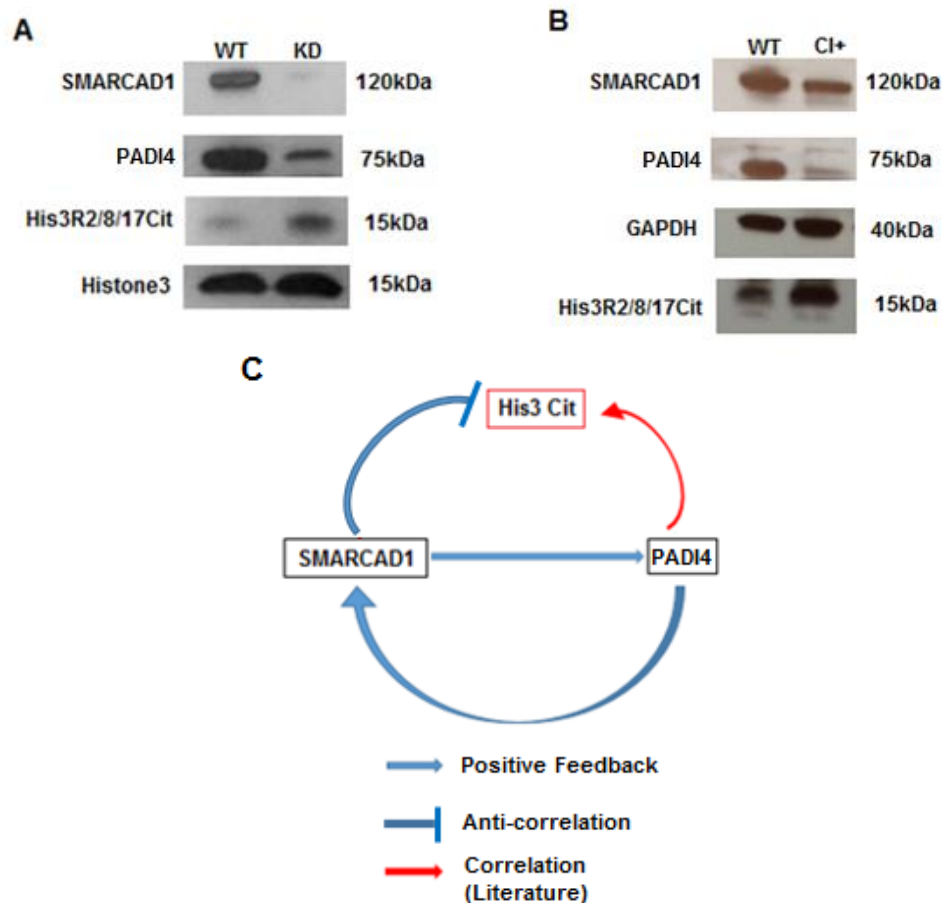


Figure 5: Protein analysis of PADI4 in mouse ES WT, KD and CI+ cells, and potential relationship between SMARCAD1, PADI4 and Histone3 citrullination. (A) SMARCAD1, His3R2/8/17Cit and Histone3 showed same result with the previous protein analysis. PADI4 protein level was lower in KD cells comparing to WT cells. (B) CI+ cells showed lower protein expression in SMARCAD1 and PADI4 comparing to WT cells, but His3R2/8/17Cit protein level was higher for CI+ sample. (C) Potential network between SMARCAD1, PADI4, and histone 3 citrullination. Positive feedback loop exists between SMARCAD1 and PADI4, and negative correlation exists between this loop and Histone3 citrullination. However based on the literature, positive correlation exists between PADI4 and histone 3 citrullination, specifically His3R2/8/17Cit.

Low protein expression level of SMARCAD1 in human kidney cancer cells comparing to non-cancer kidney cells, and existence of negative correlation between SMARCAD1 and histone 3 citrullination protein level in human kidney cells

After determining the negative correlation between SMARCAD1 and histone citrulline protein level in mouse ES cells, the next step was to ask whether the same negative correlation exists in human cells as well. Kidney cell lines were chosen because of their unique SMARCAD1 protein expression level in cancer and non-cancer tissues.

SMARCAD1 protein expression level was first tested in human kidney cancer cells 786-0 and non-cancer cells HEK-293T; both cell lines are derived from human embryonic kidney and have epithelial morphology. As expected, 786-0 showed very low level of SMARCAD1 protein expression comparing to HEK-293T based on the Western blot result (Figure 6A). Two more kidney cancer cell lines, A-498 carcinoma cell line and ACHN renal cell adenocarcinoma cell line were further tested to confirm the low expression level of SMARCAD1 gene in human kidney cancer cells comparing to non-cancer kidney cells (Figure 6B). Both A-498 and ACHN cell lines have epithelial morphology just like 786-0 and HEK-293T cells. As shown in Figure 6B, A-498 and ACHN display obvious low SMARCAD1 protein expression level comparing to HEK-293T cells, while the inner control GAPDH showed same protein expression level. In this way, we could confirmed that without any treatment or modification of the cell lines, human kidney cancer cells exhibited low protein expression level of SMARCAD1 gene in nature.

Going back to the hypothesis that decrement in SMARCAD1 protein expression leads to an increment in the protein level of histone 3 citrullination, all of the protein samples for human kidney cell lines (HEK-293T, 786-0, A-498 and ACHN) were then tested for His3CitR2/8/17 along with PADI4. All tests were performed under the same conditions of the ones for the mouse samples. As expected, all three human kidney cancer cell lines with low SMARCAD1 protein level showed very high histone 3 citrullination then HEK-293T cells (Figure 6B). There was no significant difference for the PADI4 protein expression level among human cells with different SMARCAD1 protein level (Figure 6B); this was somewhat expected because literature showed that great amount of PADI protein should be present in cancer cells [4].

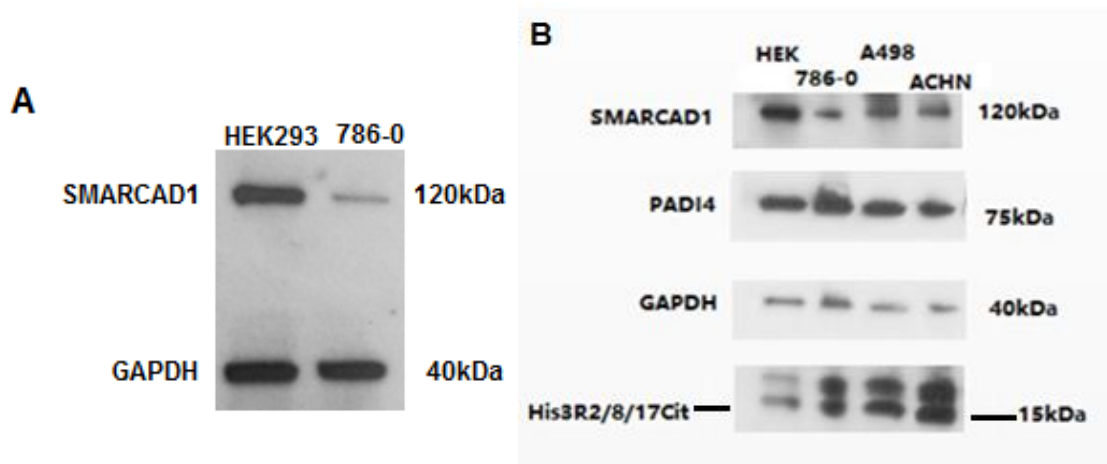


Figure 6: Protein analysis of SMARCAD1, GAPDH, PADI4, and His3R2/8/17 in human non-cancer kidney cells and human kidney cell lines. (A) Analysis of SMARCAD1 protein expression level in HEK-293T cells and 786-0 kidney cancer cells. SMARCAD1 was detected at 120 kDa, and GAPDH was detected at 40 kDa. (B) Evaluation of SMARCAD1, PADI4 and HIS3R2/8/17Cit protein expression levels in HEK-293T, 786-0, A-498 and ACHN cell lines. All three kidney cancer cell lines 786-0, A-498, and ACHN showed similar protein expression levels. All cancer lines expressed lower SMARCAD1 protein but higher His3R2/8/17Cit. Difference between PADI4 protein levels for cancer and non-cancer cell lines was not very obvious in this case. PADI4 protein levels were expected to be high in cancer cells based on the literature [4].

CRISPR/Cas9 knockout of SMARCAD1 gene in HEK-293T non-cancer kidney cell line

In order to test the potential role of SMARCAD1 gene plays in causing kidney cancer, the newly developed genome editing technique CRISPR/Cas9 system was introduced to knockout the entire SMARCAD1 gene. Because SMARCAD1 is a large gene containing 83,685 bases (from chromosome 4 position 94207608 to 94291292), SMARCAD1 KO plasmid incorporating GFP marker and SMARCAD1 HDR plasmid incorporating puromycin resistance gene and RFP marker were co-transfected to get clean knockout of SMARCAD1 and stable cell line with puromycin selection (Figure 7, Figure 8). Images were taken after 24 and 48 hours of co-transfection, and on the fourth day after puromycin selection (day 6).

This CRISPR/Cas9 gene knockout system was first performed on non-cancer HEK-293T cell lines followed the timeline shown in Figure 9A. Successful and high transfection rate was obtain for the non-cancer HEK-293T cell line. Strong GFP markers were presented in most of the cells and cell survival rate was high after puromycin selection (Figure 9B). RFP images accidentally went missing during the selection process, but both protein and RNA analysis were then performed on HEK-293T KO cells to examine the successful knocking out of SMARDAD1. Most of the cells lost their flat shape and obtained single, circular shape. Optimal number of surviving cells were allowed to grow for six more days after the selection, with normal growth medium. Cells passage was performed once before extraction of both protein and total RNA samples.

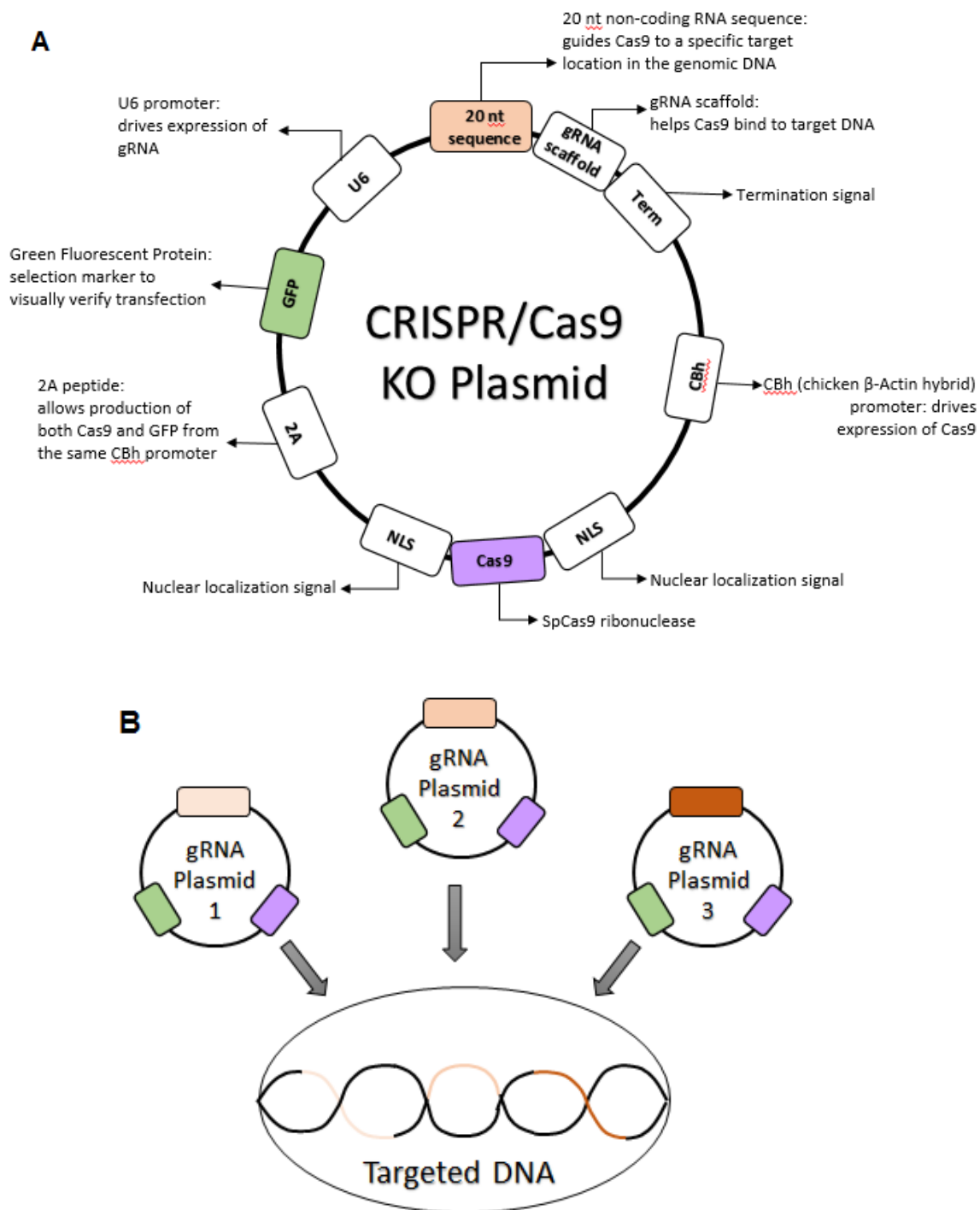


Figure 7: SMARCAD1 CRISPR/Cas9 KO Plasmid. (A) SMARCAD1 CRISPR/Cas9 KO plasmid consists of Cas9 nuclease and a SMARCAD1-specific 20 nt guide RNA (gRNA). It also has Green Fluorescent Protein (GFP) selection marker to visually verify successful transfection. (B) Each SMARCAD1 CRISPR/Cas9 KO plasmid consists of a pool of 3 plasmids with 3 gRNA designed to get the maximum CRISPR/Cas9 knockout efficiency [11].

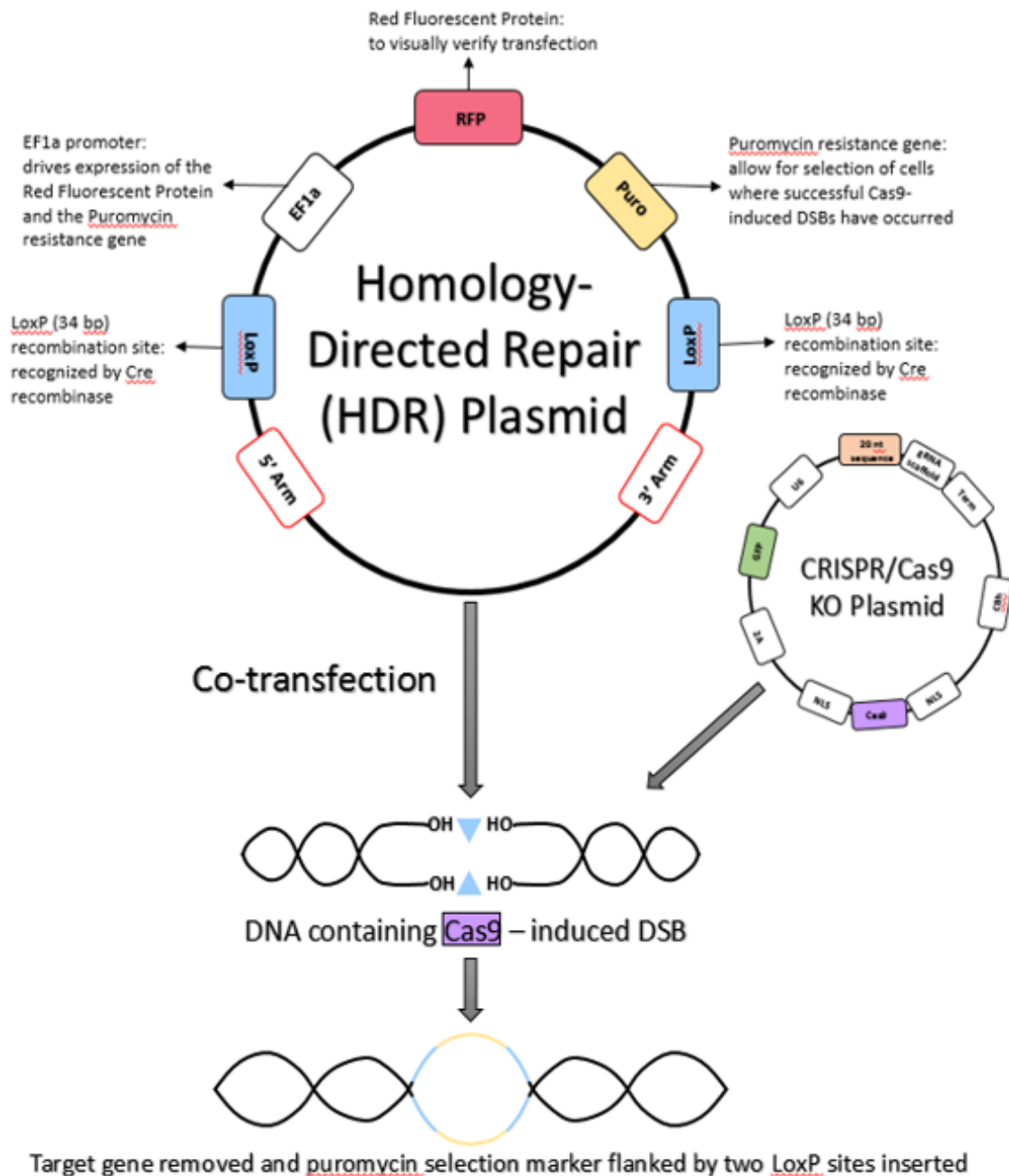


Figure 8: SMARCAD1 CRISPR/Cas9 HDR Plasmid. SMARCAD1 Homology-Directed Repair (HDR) plasmid is designed to repair the DNA containing double-strand breaks (DSB) created by the CRISPR/Cas9 system. During this repair, the SMARCAD1 HDR plasmid incorporates a puromycin resistance gene to enable selection of stable KO cells and an RFP gene to visually confirm transfection [12]. The HDR plasmid also consists of a pool of 3 plasmids specific to the break sites created by the corresponding CRISPR/Cas9 SMARCAD1 KO Plasmid, and in this way, the SMARCAD1 HDR plasmid provide a specific DNA repair template for the DSB created by the CRISPR/Cas9 SAMRCAD1 KO plasmid [12].

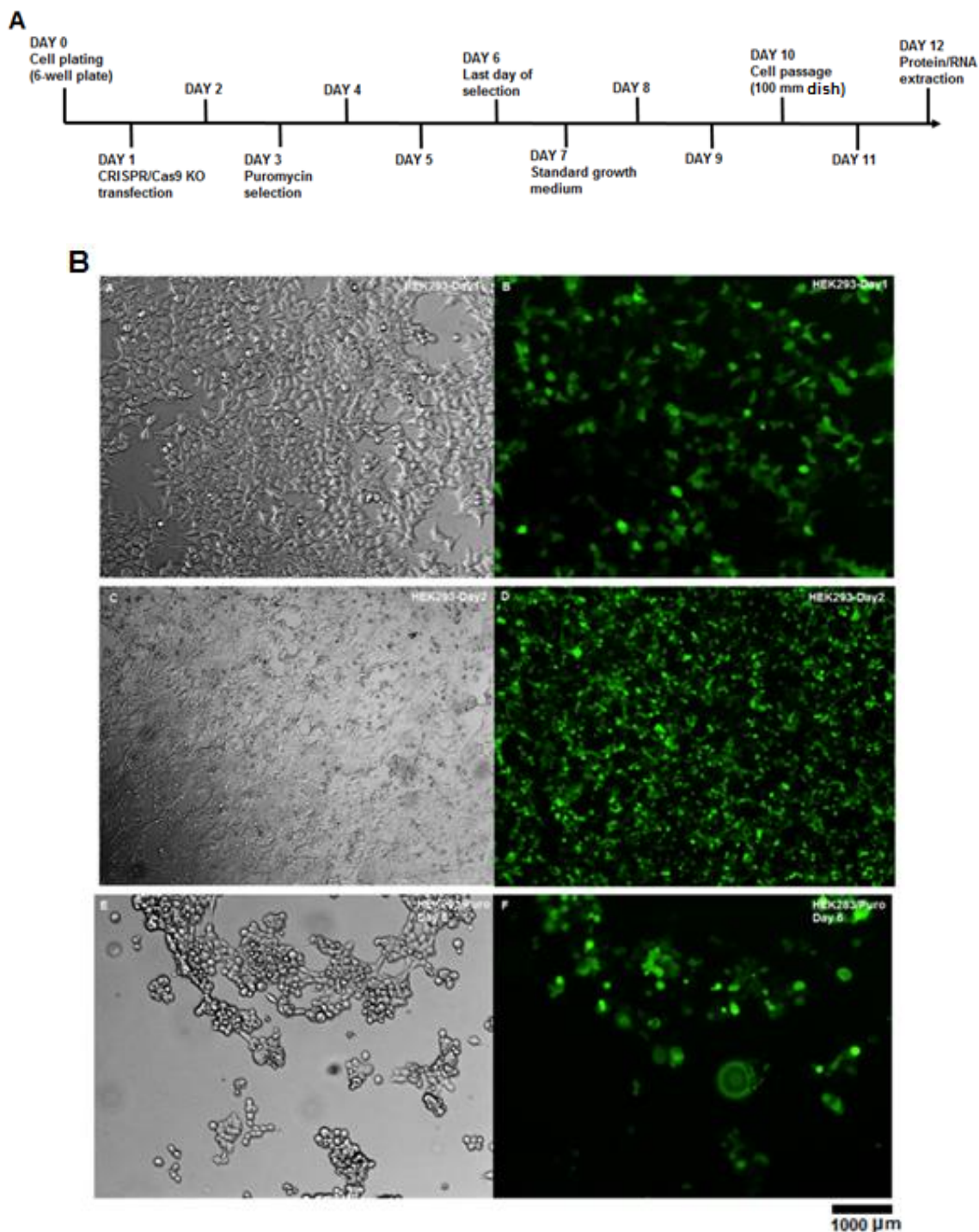


Figure 9: CRISPR/Cas9 KO/HDR co-transfection of HEK-293T kidney cells. (A) Timeline for CRISPR/Cas9 KO/HDR co-transfection of HEK-293T cells. Cells went through 6 days of transfection and selection, and 4 more days of standard maintaining. Protein and RNA of HEK-293T KO cells were extracted on day 10. (B) Bright field and GFP images for 786-0 CRISPR/Cas9 KO transfection. Images were taken on the first two days after the transfection, and on day 6, the last day of puromycin selection. The initial transfection rate was comparably high, and the rate increased dramatically after one day of incubation. Moderate amount of cells survived after 4 days of selection, and most of the surviving cells contained KO GFP markers.

Total RNA samples was extracted from control and KO HEK-293T cells for RT-PCR analysis with predesigned primers targeting SMARCAD1, GAPDH, and PADI4. The SMARCAD1 primer set was designed to specifically target the HDR recombinase region that repaired the genomic DNA cutting created by Cas9 (Figure 10). As shown in Figure 11A, low MW DNA ladder was loaded in lane M, followed by same amount (20 µg) of HEK-293T and HEK-293T KO samples in lane 1 and 2 for SMARCAD1 amplified RT-PCR products. There was a clear decrease in SMARCAD1 RNA expression level in KO sample comparing to wildtype HEK-293T sample. Small amount of SMARCAD1 gene still presented in the HEK-293T KO cells because single cell cloning had not been performed, and the sample was from a heterogeneous cell pool. Lane 5 and 6, and lane 9 and 10 in Figure 11A were loaded with amplified GAPDH and PADI4 products correspondingly, and there were no RNA expression change for both genes between the samples. Consistent RNA level of PADI4 indicated that the potential positive feedback between SMARCAD1 and PADI4 might only appear on the protein level and there might be factors during the translation process that lead to this correlation. Quantitative RT-PCR (qRT-PCR) was also done on both WT and KO RNAs to detect the actual numerical change of SMARCAD1 RNA level. GAPDH was used as a control and its RNA level remained about the same level in both WT and KO HEK-293T cells (Graph 1). SMARCAD1 RNA level dropped to 0.31683314 of the original RNA level in HEK-293T KO cells. This was in parallel with the gel image in Figure 11A, and proved a high efficiency of the CRISPR/Cas9 knockout of SMARCAD1 gene in HEK-293T cells.

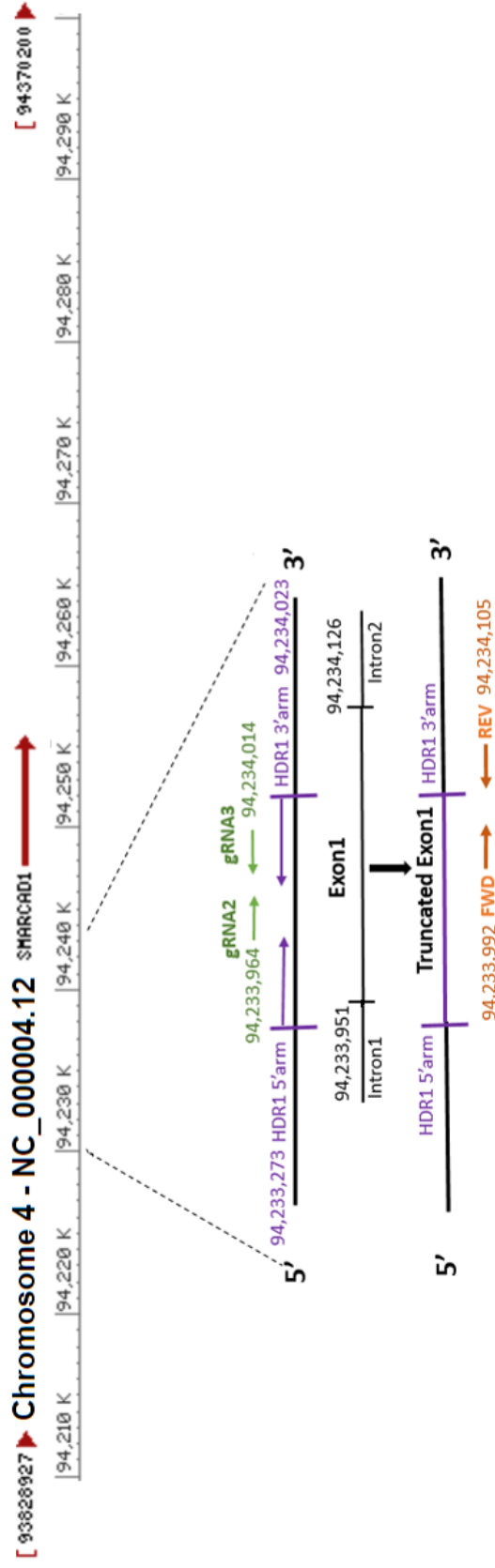


Figure 10: SMARCD1 primer set targeting HDR recombinase region. The SMARCD1 primers were designed to specifically target the cutting region that had been repaired by the HDR plasmid.

Protein samples were also extracted on the same day as the RNA samples and Western blot was performed. As shown in Figure 11B, HEK-293T KO sample showed no SMARCAD1 protein expression at all. This missing band even with a longer exposure time indicated that CRISPR/Cas9 knockout was very efficient. Again, there was no change in expression level for the housekeeping gene GAPDH (Figure 11B). Together with the RNA analysis, it was confirmed that CRISPR/Cas9 knocking out of SMARCAD1 gene was successful in HEK cells.

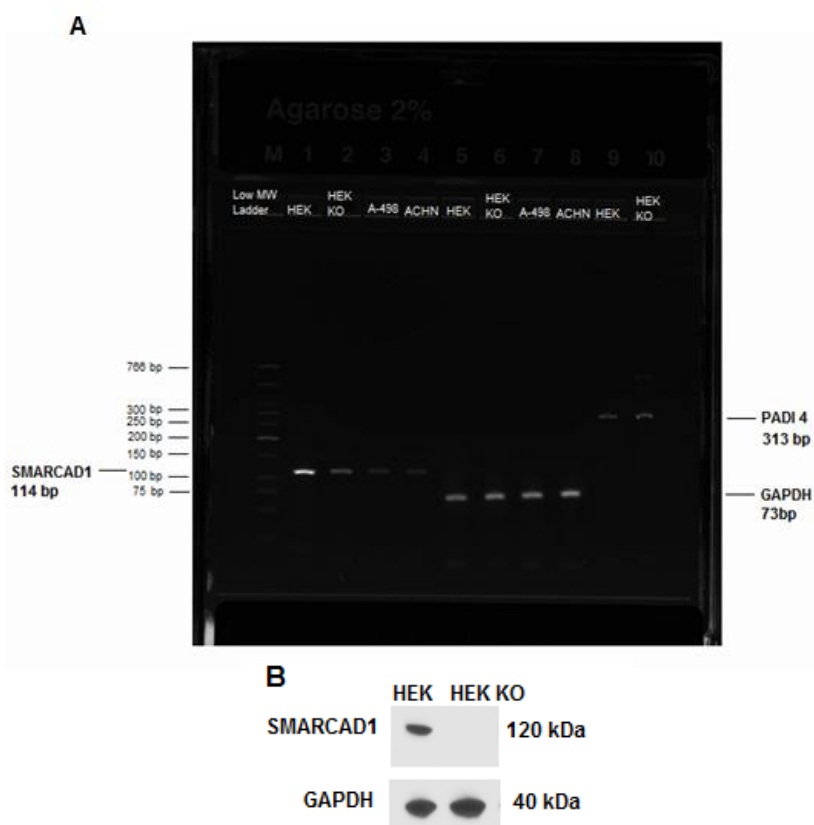


Figure 11: RNA and Protein Analysis of HEK-293T and HEK-293T KO Cells on SMARCAD1 expression level. (A) Gel electrophoresis of SMARCAD1 RNA expression level in wildtype HEK-293T and HEK-293T KO cells. Amplified SMARCAD1 products were observed at 114bp. Low MW DNA ladder was loaded in to lane M. GAPDH (73bp) was used as an internal control and the RNA expression was consistent for all for samples. Wildtype HEK-293T expressed a significant amount of SMARCAD1 RNA comparing to HEK-293T KO cells. There was no difference between HEK-293T and HEK-293T KO for PADI4 (313bp) RNA expression level. (B). Western blot protein analysis for CRISPR/Cas9 knockout of SMARCAD1 gene in HEK-293T cells. SMARCAD1 protein was detected at 120kDa in wildtype HEK-293T, but there was no detection in KO sample, which indicated a successful CRISPR/Cas9 knockout transfection. GAPDH protein expression level was consistent in both samples.

CRISPR/Cas9 knockout of SMARCAD1 gene in kidney cancer cell lines: 786-0, A-498 and ACHN

CRISPR/Cas9 knockout was then performed on the kidney cancer cell lines. 786-0 cell line was in fact transfected at the same with HEK-293T cells followed the timeline shown in Figure 12A. However, 786-0 showed a very low transfection rate. After puromycin selection, there was little cell left with almost no GFP marker (Figure 12B). Transfected cells were allowed to grow for four more days with regular growth medium, but no cell survived at the end and CRISPR/Cas9 knockout transfection failed in 786-0 cell line.

Due to the unsuccessful transfection in 786-0 cells, it was then performed on the other kidney cancer cell lines, A-498 and ACHN, and the complete process took 20 days in total (Figure 13). Compare to 786-0 cells, optimal results were obtained for both cancer cell lines; still, the transfection efficiency was much lower than the one for HEK-293T cells. This might due to the difficulty of CRISPR-Cas9 delivery in cancer cell lines. Both cell lines went through 4 days of puromycin selection and at day 6, there were still cells presented with CRISPR/Cas9 KO cutting marker GFP and HDR marker RFP (Figure 14, Figure 15). Since the available cell amount for both cancer cell lines was limited after the puromycin selection, A-498 and ACHN were allowed to grow in a smaller well plate for nine more days. Fluorescence images were taken on day 12 and day 15 (Figure 16A, Figure 16B) before passing into larger well plates. Both total RNA and protein samples were then extracted on the same day to determine the CRISPR/Cas9 knockout efficiency.

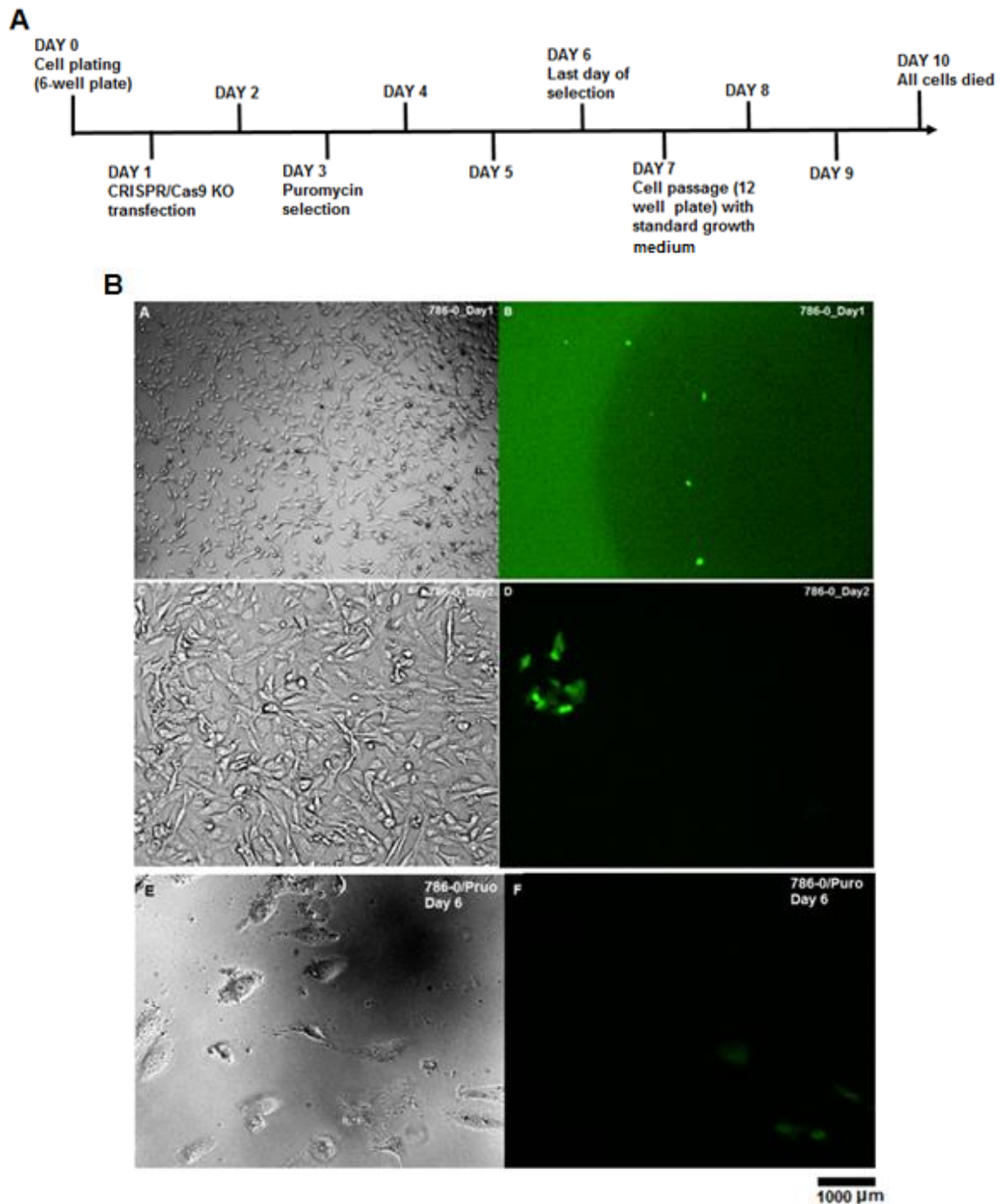


Figure 12: CRISPR/Cas9 KO/HDR co-transfection of 786-0 kidney cancer cell line. (A) Timeline for CRISPR/Cas9 KO/HDR co-transfection of 786-0 cells. Cells went through 6 days of transfection and selection, and six more days of standard cell maintenance. However all remaining cells after selection died on day 12. (B) Bright field and GFP images for 786-0 CRISPR/Cas9 KO transfection. Images were taken on the first two days after the transfection, and on day 6, the last day of puromycin selection. The initial transfection rate was very low, and only a few cell survived with KO GFP marker after 4 days of selection.

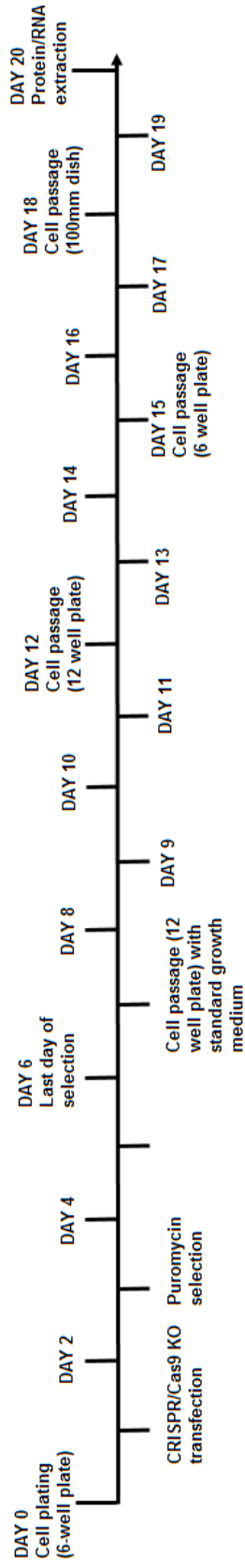


Figure 13: Timeline of CRISPR/Cas9 KO/HDR co-transfection of A-498 and ACHN kidney cancer cell lines. Both A-498 and ACHN cells went through 6 days of transfection and selection, and 14 more days of standard cell maintenance due to the small amount of selected KO cells. Protein and RNA of both A-498 KO and ACHN KO cells were extracted on day 20.

RT-PCR was done on both A-498 and ACHN total RNA samples with the same SMARCAD1 and GAPDH primers that was used for HEK-293T cells. All amplified samples were run on an agarose gel and both KO samples showed lower RNA expression comparing to their wildtype samples (Figure 17A). This SMARCAD1 expression change was not as obvious as the one in HEK-293T cells. However, A-498 and ACHN samples in nature showed lower SMARCAD1 RNA expression level than HEK-293T as expected from the literature (Figure 11A, Lane 1-4). QRT-PCR numerical results showed that both RNA levels did decrease. A-498 KO cells dropped to 0.67279101 of its SMARCAD1 RNA level in WT cells, and ACHN KO cells dropped to 0.659803956. The CRISPR/Cas9 knockout efficiencies were not very high in both kidney cancer lines. Agarose gel and QRT-PCR results all indicated a consistent RNA expression for amplified GAPDH RT-PCR products in A-498, A-498 KO, ACHN and ACHN-KO samples (Figure 17A, Graph 1).

Western blot result also confirmed the success of CRISPR/Cas9 knockout of SMARCAD1 gene in A-498 and ACHN. Both wildtype A-498 and ACHN showed low SMARCAD1 protein expression as before; while A-498 KO and ACHN KO samples showed no SMARCAD1 protein band (Figure 17B). This indicated efficient CRISPR/Cas9 knockout of SMARCAD1 in both kidney cancer cell lines. All bands for the inner control GAPDH showed same protein expression level (Figure 17B). Together with the RNA analysis, it was confirmed that CRISPR/Cas9 knocking out of SMARCAD1 gene was successful in A-498 and ACHN cell lines. However, the transfection rate was still lower than the one for non-cancer HEK-293T cells.

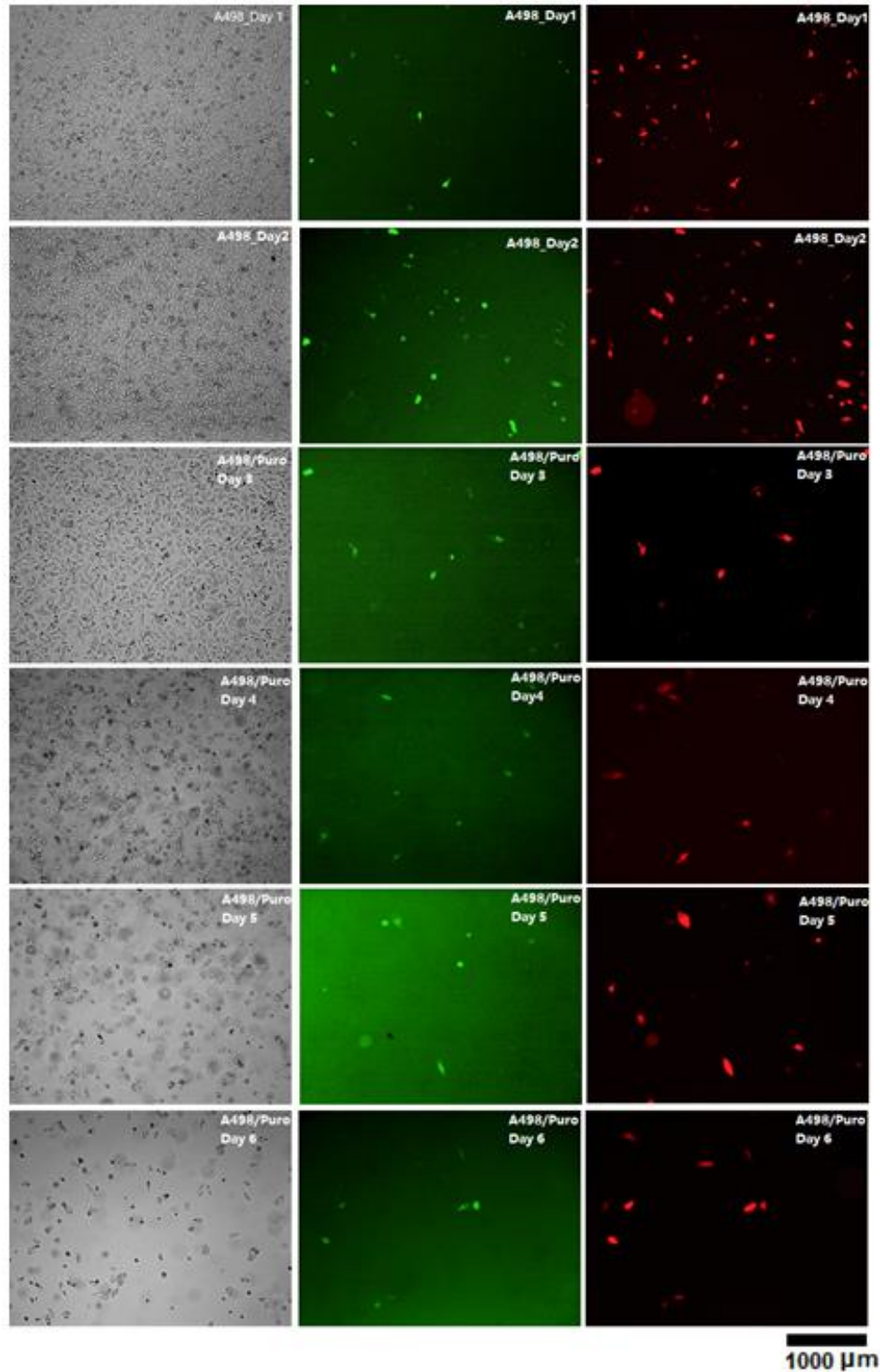


Figure 14: CRISPR/Cas9 KO/HDR co-transfection of A-498 kidney cancer cells. Bright field, GFP and RFP images were taken from Day 1 of the transfection to Day 6, the end of puromycin selection. Transfection rate was low comparing to HEK -293T cells. After 4 days of selection, small amount of cells survived with KO/HDR markers. While the amount was sufficient for continued culture and analysis.

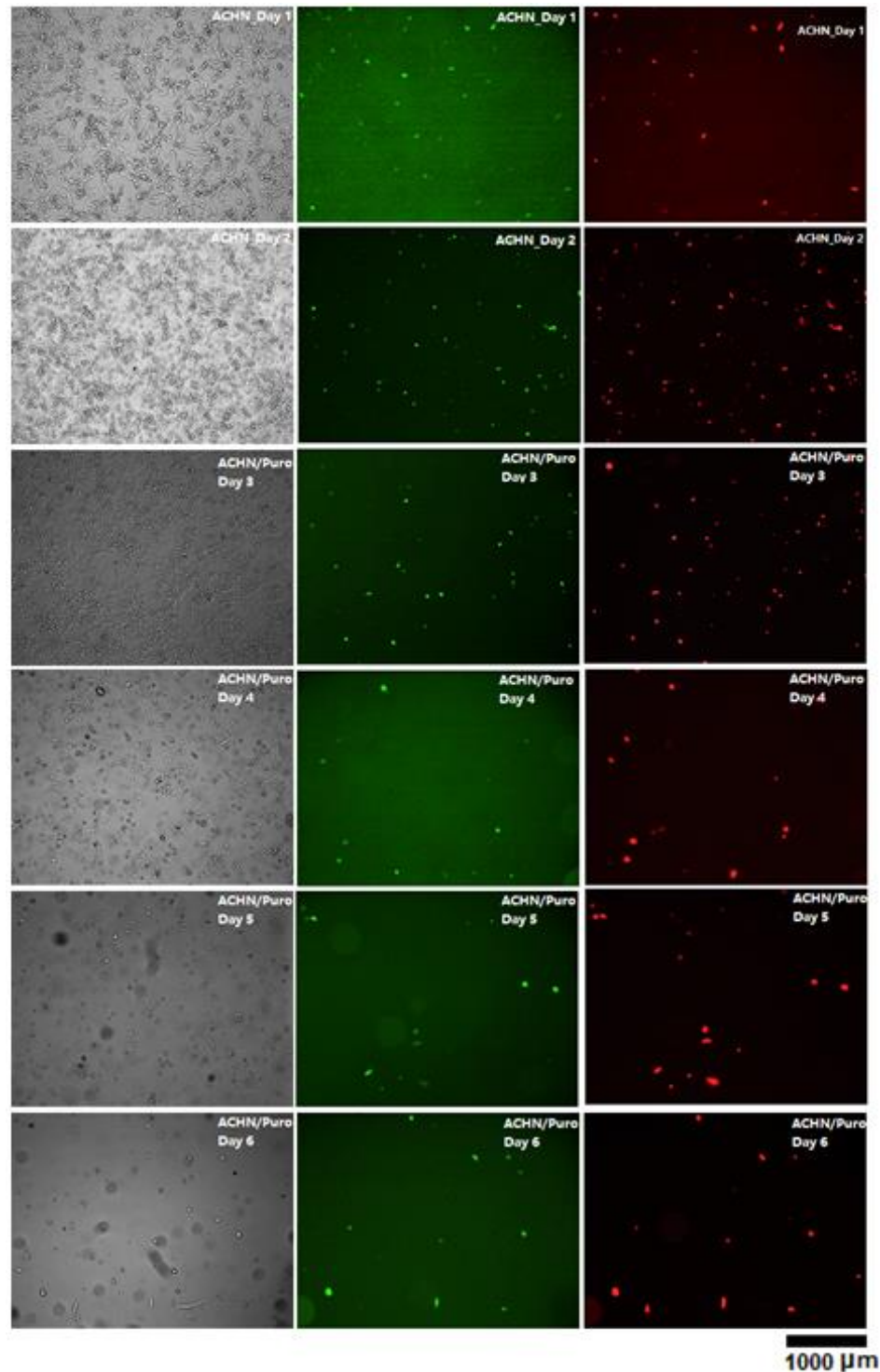


Figure 15: CRISPR/Cas9 KO/HDR co-transfection of ACHN kidney cancer cells. Bright field, GFP and RFP images were taken from Day 1 of the transfection to Day 6, the end of puromycin selection. Transfection rate was also low comparing to HEK-293T cells. Similar to A-498 cells, after 4 days of selection, small amount of cells survived with KO/HDR markers. While the amount was sufficient for continued culture and analysis.

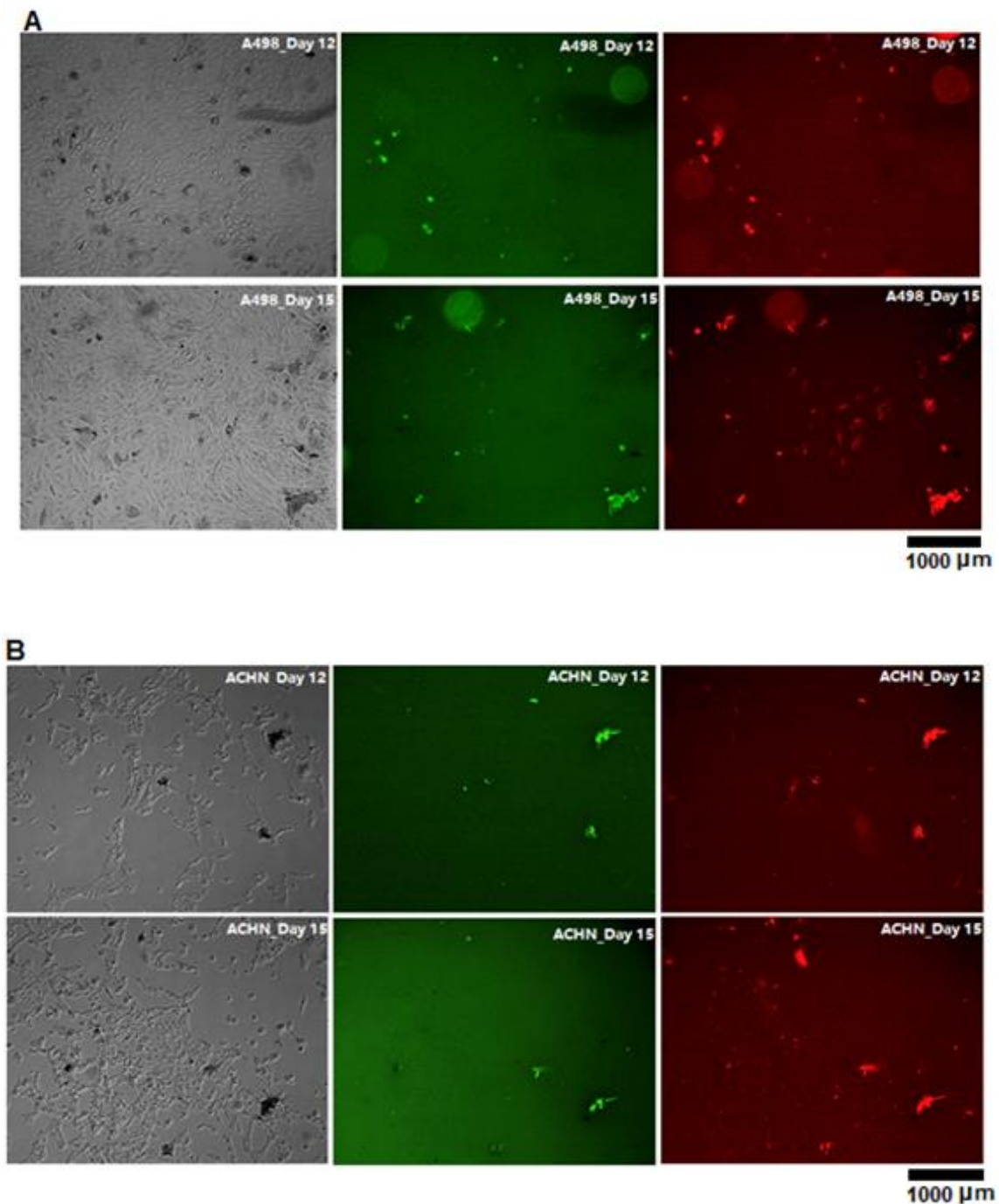


Figure 16: Standard cell maintenance of A-498 and ACHN KO cells after CRISPR/Cas9 KO co-transfection. (A) Bright field, GFP and RFP images of A-498 KO cells on Day 12 and Day 15. KO cells remained healthy growth, but the transfection rate was low. Transfection rate of HDR plasmid with RFP and puromycin markers was higher than KO plasmid with GFP marker (B) Bright field, GFP and RFP images of ACHN KO cells on Day 12 and Day 15. The growth rate was lower than A-498 KO cells. While the transfection rate was around the same with A-498 KO cells. Transfection rate of HDR plasmid with RFP and puromycin markers was higher than KO plasmid.

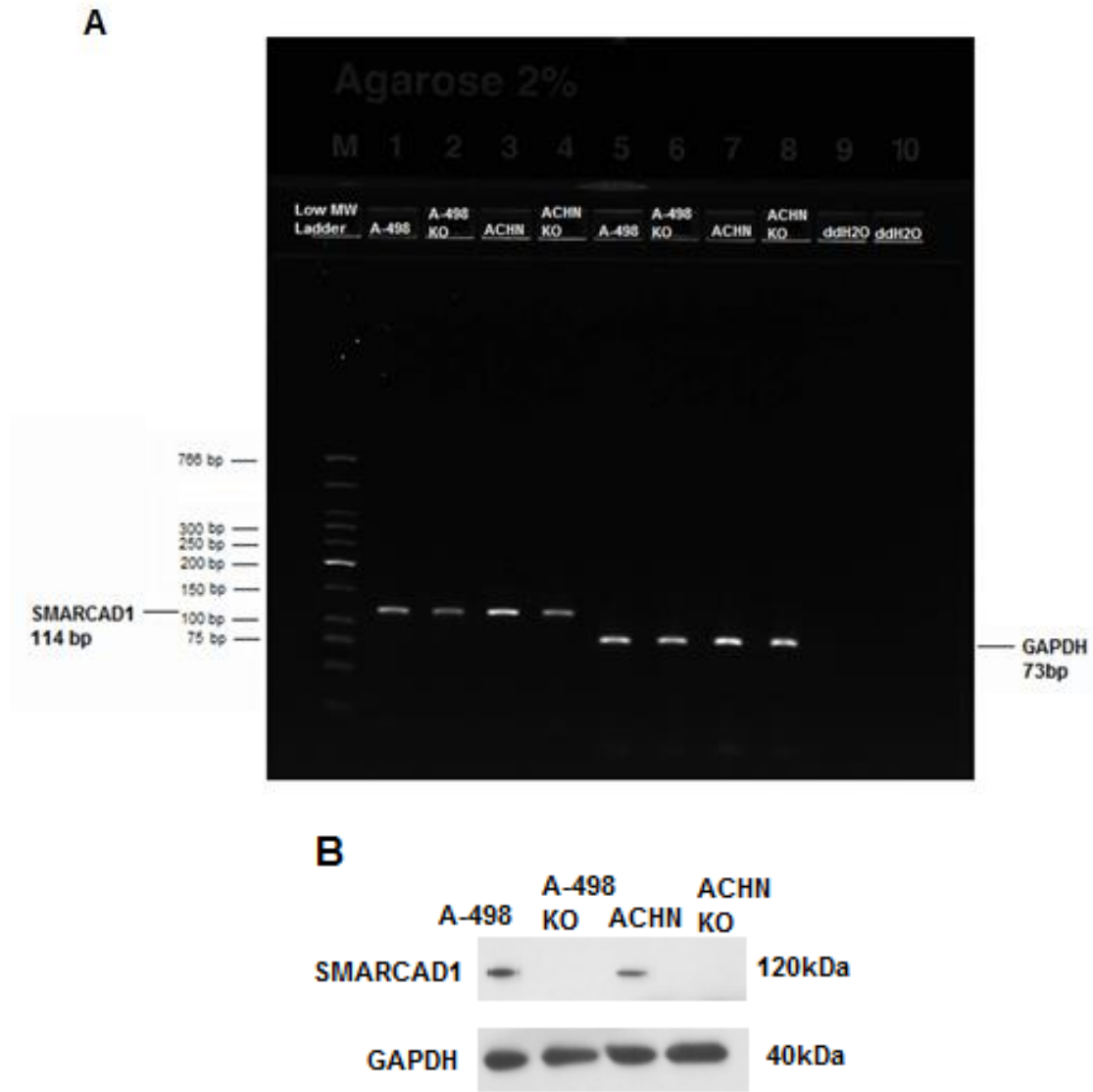
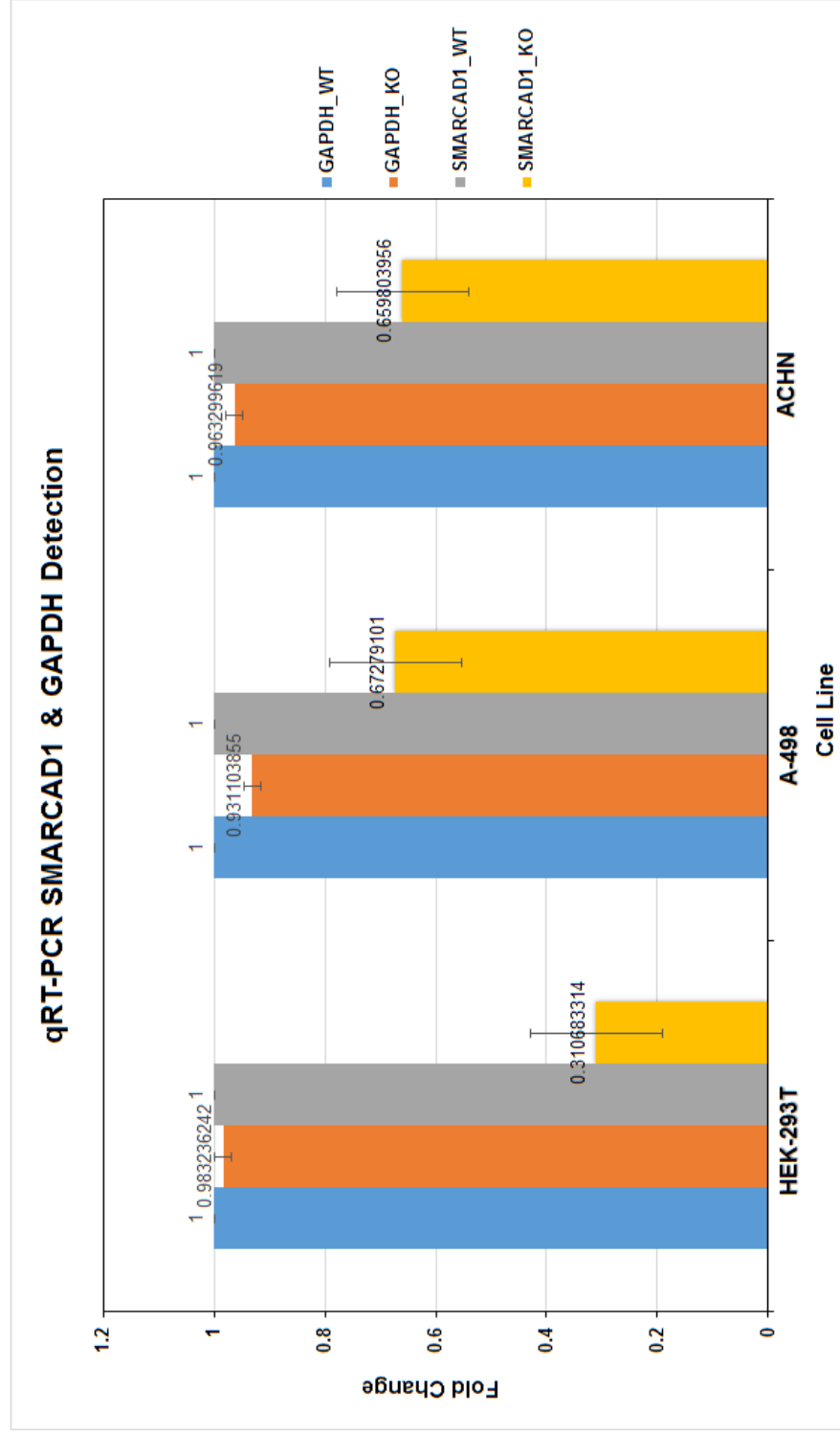


Figure 17: RNA and Protein Analysis of A-498, A-498 KO, ACHN and ACHN KO cells on SMARCAD1 expression level. (A) Gel electrophoresis of SMARCAD1 RNA expression level in wildtype A-498, A-498 KO, wildtype ACHN and ACHN KO cells. Amplified SMARCAD1 products were all observed at 114bp. Low MW DNA ladder was loaded in to lane M. GAPDH (73bp) was used as an internal control and the RNA expression was consistent for all for samples. Both wildtype A-498 and ACHN expressed higher amount of SMARCAD1 RNA comparing to their corresponding KO samples, indicated efficient knocking out of SMARCD1 gene. Because KO samples were extracted from heterogeneous cell pools, low amount of SMARCAD1 RNA still existed for both cell lines (B). Western blot protein analysis for CRISPR/Cas9 knockout of SMARCAD1 gene in A-498 and ACHN cells. SMARCAD1 protein was detected at 120kDa in both wildtype cells, but there was no detection in KO sample, which indicated a successful CRSIPR/Cas9 knockout transfection. GAPDH protein expression level was consistent in all samples.

Graph 1: qRT-PCR results of SMARCAD1 and GAPDH RNA fold change in WT and KO HEK-293T, A-498 and ACHN cell lines. Fold changes of SMARCAD1 and GAPDH were calculated for all WT and KO cells. GAPDH RNA detection level remained mostly consistent for all three kidney cell lines. For HEK-293T KO cells, SMARCAD1 RNA level reduced to about 0.31 of the original RNA level in WT cells. For both kidney cancer KO cells, RNA level dropped to around 2/3 of the original RNA level in corresponding WT cells. HEK-293T presented a much higher CRISPR/Cas9 knockout efficiency.



Negative correlation between SMARCAD1 and Histon3 citrullination with Positive Feedback between SMARCAD1 and PADI4 in HEK-293T Cells

The next step was to determine if modification of SMARCAD1 gene actually modulate the protein expression level of His3R2/8/17Cit and PADI4. Wildtype HEK-293T and HEK-293T KO protein samples were analyzed again with SMARCAD1, PADI4, and His3R2/8/17Cit antibodies. Figure 18 shows that with a clear knocking out of the SMARCAD1 gene in the protein level, His3R2/8/17Cit did show an increased protein expression level in HEK-293T KO cells, which suggested the negative correlation between SMARCAD1 and His3R2/8/17Cit. GAPDH inner control did not change between HEK-293T and HEK-293T KO, which showed that this protein analysis was valid.

Compare to HEK-293T, HEK-293T KO sample also had a slightly lower PADI4 protein level (Figure 18A), which led to the examining of potential positive feedback loop between SMARCAD1 and PADI4. HEK-293T cells were treated with Cl-amidine followed the exact condition for the mouse cells. HEK-293T Cl+ sample was then analyzed with HEK. The anticipated positive feedback turned out to be true. With very low protein level of PADI4 for HEK-293T Cl+ sample, SMARCAD1 showed a slight decreased protein level as well and His3R2/8/17Cit protein level went up for HEK-293T Cl+ sample (Figure 18B). These observations again suggested the network between SMARCAD1, PADI4, and His3R2/8/17Cit (Figure 18C). With a positive feedback loop connecting SMARCAD1 and PADI4, a decrement in one of them will cause an increment in the His3R2/8/17Cit protein expression level.

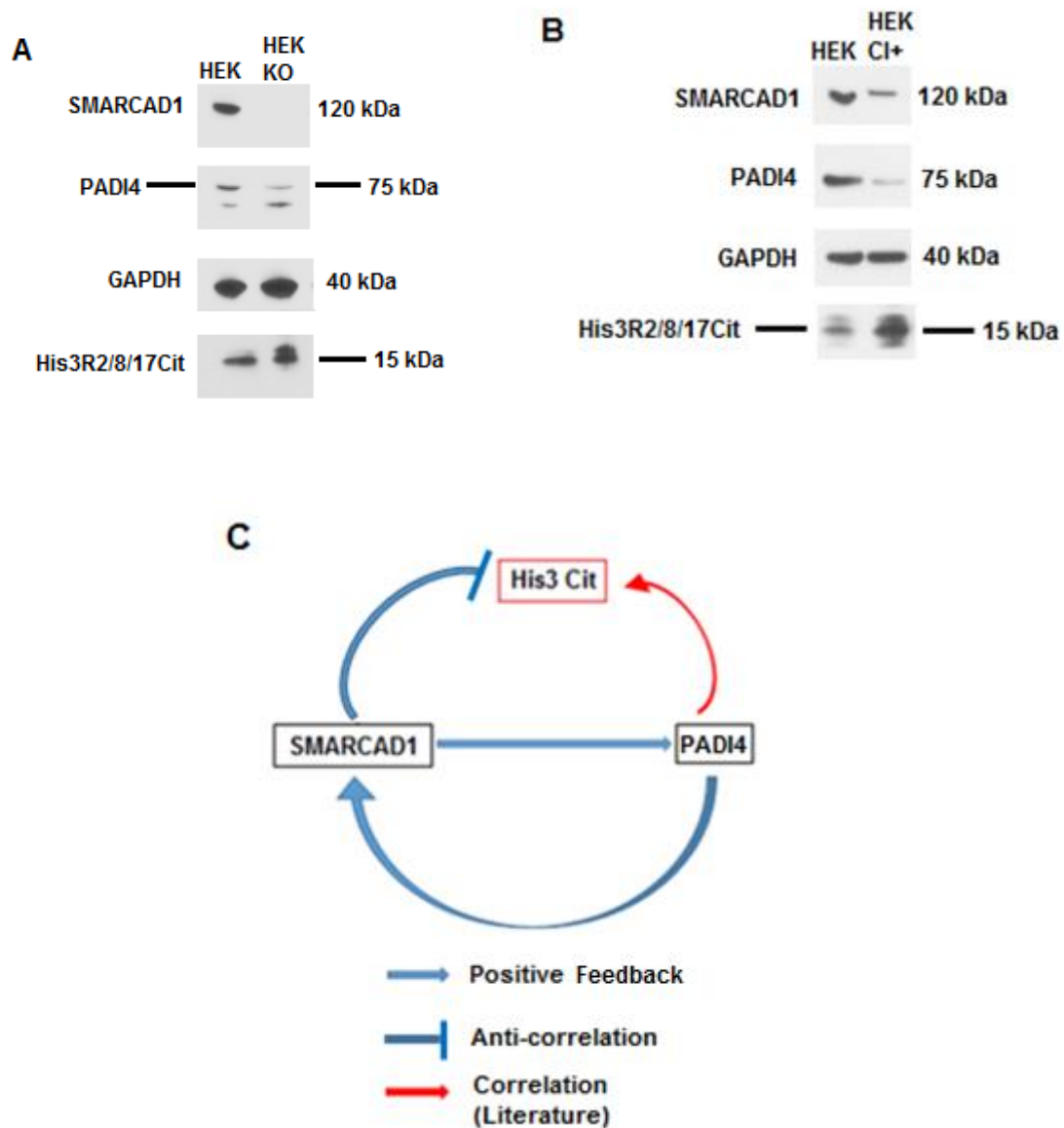


Figure 18: Protein analysis of His3R2/8/17Cit and PADI4 in HEK-293T, HEK-293T KO and HEK-293T CI+ cells, and potential relationship between SMARCAD1, PADI4 and Histone3 citrullination. (A) SMARCAD1 and His3R2/8/17Cit showed consistent result with the previous protein analysis for HEK-293T and HEK-293T KO cells. PADI4 protein level was slightly lower in KO cells comparing to wildtype cells. (B) HEK-293T CI+ sample showed lower protein expression in SMARCAD1 and PADI4 comparing to wildtype HEK-293T cells, but His3R2/8/17Cit protein level was higher for CI+ sample. (C) Potential network between SMARCAD1, PADI4, and Histone3 citrullination. Same positive feedback loop exists between SMARCAD1 and PADI4 in human kidney cells like the one for mouse ES cells. Negative correlation exists between this loop and Histone3 citrullination based on the protein analysis. Again, literature states a positive correlation between PADI4 and Histone3 citrullination, specifically His3R2/8/17Cit.

Negative correlation between SMARCAD1 and Histon 3 Citrullination in Kidney Cancer Cells

Lastly, histone 3 citrulline protein level was tested on CRISPR/Cas9 KO cancer cells to confirm the negative correlation between SMARCAD1 and citrullination existed in kidney cancer. As shown in Figure 19, with consistent protein expression of inner control GAPDH and clear knocking out of SMARCAD1, both A-498 and ACHN KO cells had much higher His3R2/8/17Cit protein expression than their corresponding wildtype cells. Due to the limited protein amount (7 μ g), it was hard to see the His3R2/8/17Cit expression for A-498 cells; still, the original film showed extremely lower amount of His3R2/8/17Cit comparing to the A-498 KO cells. This indicated that the negative correlation did exist in not only mouse ES cells, but also human non-cancerous and cancer cells. The difference between PADI4 protein level in each wildtype and KO cancer cell line was not very significant. This might due to the higher protein level of PADI4 in cancerous cells in nature [4], and complex growth mechanisms for cancer cells. However, both kidney cancer cell lines expressed slightly lower amount of PADI4 comparing to their wildtype cells.

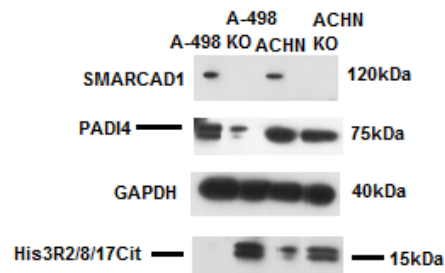


Figure 19: Protein analysis of His3R2/8/17Cit in A-498 and ACHN WT and KO cells. Both KO kidney cancer cell lines showed higher His3R2/8/17Cit protein expression. Difference between PADI4 protein levels were not very significant. Inner control GAPDH had consistent protein level and SMARCAD1 was clearly knocked out from both kidney cancer cell lines.

Material and Methods

Cell culture

Mouse embryonic stem (ES) cells and SMARCAD1 knockdown cells (#2) were cultured in embryonic stem cell (ES) medium (Reid) with daily fresh medium change. Human HEK-293T cells were maintained in DMEM medium (ATCC, 30-2002) with 1% FBS (Gemini, 100-500) and 1% Penicillin-Streptomycin (Gibco, 15140122). All three kidney cancer cell lines 786-0, A-498, and ACHN were purchased directly from ATCC and maintained in RPMI-1640 medium (ATCC, 30-2001) with 10% FBS. All kidney cancer cell lines required fresh medium change every 2-3 days.

RNA knockdown of mouse ES cells

One shRNA targeting the mouse SMARCAD1 mRNA with puromycin selection marker, which was pre-constructed by the senior research associate, was used to knockdown the SMARCAD1 RNA in ES cells. The shRNA sequence was GTATGAGGATTACAATGTA. ES cells were transfected with this shRNA constructs by Lipofectamine 2000 (Invitrogen, 11668030) followed by Puromycin (Sigma, P9620) selection for 3 days. The protein was extracted on Day 4 after the puromycin selection.

PADI inhibition treatment

Mouse ES cells and Human HEK-293T cells were treated with Cl-amidine (Calbiochem, 506282), a cell-permeable pan PAD inhibitor for 3 days with standard ES medium and HEK-293T medium (DMEM medium with 1% FBS). The Cl-amidine was dissolved in 1ml of Dimethyl sulfoxide (Sigma, 2650) to make a final

concentration of 10 mg/ml working solution. Fresh medium was change daily with 0.84 mg/ml of CI-amidine added into the medium. Medium change was performed for three days, and all protein samples were extracted on Day 4 of the CI-amidine treatment.

Western Blot

Proteins were extracted from the adhesion cells using RIPA buffer (Cell Signaling, 9806) with EDTA-free Protease Inhibitor (Sigma, 4693132001). Protein concentrations (Table 1) were determined by performing BCA assay (Pierce, 23225) using a plate reader. To keep consistency, 15 μ g and 7 μ g of protein in a total loading volume of 10 μ l were used for all samples based on different protein conditions (Table 1). The proteins were transferred onto PVDF membrane (Biorad, 1620177), and then incubated with antibodies. The antibodies used were SMARCAD1 (Abcam, ab6748), GAPDH (Abcam, ab9485), PADI4/PAD4 (Abcam, ab96758), Histone H3 (Abcam, ab10799), Histone H3 citrulline R26 (Abcam, ab19847), and Histone H3 citrulline R2+R8+R17 (Abcam, ab5103). The antibodies condition is shown in Table 2.

Table 1: Protein Samples Concentration and Western Blot Loading Condition

	Protein Concentration (μ g/ μ l)	Protein Amount (μ g)	Loading	Protein Volume (μ l)	Loading
ES	3.940	15.00		3.807	
#2	4.476	15.00		3.351	
CI+	3.658	15.00		4.100	
HEK-293T	3.191	15.00		4.700	
786-0	4.386	15.00		3.420	
A-498	2.977	15.00	7.00	5.039	2.351
ACHN	3.230	15.00	7.00	4.644	2.167
HEK-293T KO	3.388	15.00		4.427	
A-498 KO	1.663	7.00		4.209	
ACHN KO	1.181	7.00		5.926	

Table 2: Primary and Secondary Antibody Dilution Condition for Western Blot on Mouse ES Cells and SMARCAD1 KD #2 Cells

	Primary Antibody	Secondary Antibody	Band Size (kDa)
Anti-SMARCAD1	1:1000	1:3000	117
Anti-PADI4	1:2000	1:3000	74
Anti-GAPDH	1:4000	1:3000	37
Anti-Histone3	1:3000	1:3000	15
Anti-H3R26Cit	1:2000	1:2000	15
Anti-H3R27/18Cit	1:2000	1:4000	15

CRISPR/Cas9 KO transfection

Commercially ready SMARCAD1 CRISPR/Cas9 KO Plasmid (Santa Cruz, sc-416238) and SMARCAD1 HDR Plasmid (Santa Cruz, sc-416238-HDR) were purchased. Both plasmids were re-suspended in 200µl of DNase-free water to make a final concentration of 0.1 µg/µl, and stored at -20°C. CRISPR KO transfection was performed followed the CRISPR KO Transfection Protocol from Santa Cruz Biotechnology. Lipofectamine 3000 (Invitrogen, L3000001) was used instead of the Santa Cruz transfection reagent.

0.5×10⁶ per well of cells were seeded onto two wells of the 6-well plates for HEK-293T, 786-0, A-498, and ACHN cells the day before the transfection. Approximately 24 hours after seeding the cells, cell grew to about 80% confluency and all cells were co-transfected with 2 µg of KO and 2 µg of HDR plasmids per well. 7.5µL of the Lipofectamine 3000 Reagent and 4 µL of P3000 Reagent were used per well during the transfection. All cells were seeded in 3 ml of corresponding standard growth medium per well.

CRISPR/Cas9 KO selection

Approximately 48 hours post-transfection, standard growth mediums were replaced with fresh mediums containing 3 µg/ml puromycin for all four cell lines.

Cell selection was then performed for 4 days with daily fresh medium change. Bright field and fluorescence images were taken every day for all four KO cell lines to record the cell growth. Selection was stopped after Day 6 and all KO cells were changed to standard growth mediums on Day 7.

Approximately 1.8525×10^5 HEK-293T KO cells per well remained in the 6-well plates and the cells were allowed to grow for three additional days before passaging each well onto 100mm tissue culture plates on Day 10; extraction of protein and total RNA was able to be performed on Day 12 with a 80% of cell confluency per well. Small amount of HEK-293T KO cells were frozen down for future research purpose.

A-498 and ACHN KO cells were passaged onto four wells of 12-well plates on Day 7. Approximately 2.024×10^4 A-498 KO cells were cultured in each well of the 12-well plates and approximately 1.334×10^4 ACHN KO cells were culture in each well of the 12-well plates. Both KO cell lines were allowed for longer period of growth due to a small amount of surviving cells after the puromycin selection. Both cell lines were passaged onto 2 wells of the 6-well plates on Day 15. KO cells were allowed to grow for three additional days before passaging each well onto 100mm tissue culture plates on Day 18. Extraction of protein and total RNA from A-498 and ACHN KO cells was able to be perform on Day 20. Small amount of A-498 KO and ACHN KO cells were frozen down for future research purpose.

RT-PCR

Total RNA was extracted from the adhesion cells using GeneJet RNA Purification Kit (Thermo Scientific, K0731). Total RNA concentrations are shown

in Table 3, and 1 μ g of each total RNA sample was used in the RT-PCR step. RT-PCR was then performed using the QIAGEN OneStep RT-PCR Kit (QIAGEN, 210210) with 35 reaction cycles. Specific cycling conditions including time and temperature for each step are shown in Table 5. Both SMARCAD1 and GAPDH primer sets were designed using NCBI Primer-BLAST and purchased from IDT. PADI4 primer set was purchased directly from ORIGENE (ORIGENE, HP210325). The primer sequences are listed in Table 4. RT-PCR products were then analyzed by performing gel electrophoresis using 2% E-Gel EX Agarose Gels (Invitrogen, G402002) with low molecular weight DNA ladder (NEB, N0557). RNA gel electrophoresis loading conditions are shown in Table 6.

qRT-PCR

Total RNA was also analyzed with two-step qRT-PCR to determine the exact fold change of RNA samples in wildtype and knockout cell lines (HEK-293T, A-498 and ACHN). Reverse transcription was performed in the first step using High-Capacity cDNA Reverse Transcription Kit (Applied Biosystems, 4368814). Reverse transcription conditions are shown in Table 7, and synthesized cDNA concentrations for each cell line are shown in Table 8. All cDNA samples were then analyzed by performing standard qRT-PCR with *Power SYBR® Green PCR Master Mix* (Applied Biosystems, 4367659), and previous primer sets. Three repeats from each cDNA sample were loaded onto a 96-well PCR plate. Table 9 shows the qRT-PCR Cycling Conditions. Cycling thresholds (Ct) were detected and average cycling threshold for each sample was calculated based on the three

repeats. Fold changes for all samples were determined based on the equation:

$2^{-\delta\delta Ct}$ (Table 10).

Table 3: Total RNA Concentrations

	Total RNA Concentration (ng/μl)	1μg of Total RNA (μl) in RT-PCR Reaction
HEK-293T	663.0	1.508
A-498	467.1	2.141
ACHN	571.9	1.749
HEK-293T KO	833.2	1.200
A-498 KO	144.0	6.944
ACHN KO	174.0	5.747

Table 4: RT-PCR Primer Sequence

Gene	Forward Primer 5'-3'	Reverse Primer 5'-3'
SMARCD1	CTACCATGGCACGTAGAAATG	CACTTCTTTGTGGAAAAAGTTCC
GPADH	AATCCCATCACCATCTTCCA	TCCTAGTTGCCTCCCCAAAG
PADI4	GCACAACATGGACTTCTACGTGG	CACGCTGTCTTGGAAACACCACA

Table 5: One-step RT-PCR Cycling Conditions

Step	Time	Temperature
Reverse Transcription	30 min	50°C
Initial PCR Activation	15 min	95°C
35 Cycles:		
Denaturation	30 sec	94°C
Annealing	30 sec	50°C
Extension	1 min	72°C
Final Extension	10 min	72°C

Table 6: RNA Gel Electrophoresis Loading Conditions

	Sample	Amount (ng)
Figure 7A	HEK-293T	20
	HEK-293T KO	20
	A-498	20
	ACHN	20
Figure 12A	A-498	50
	A-498 KO	50
	ACHN	50
	ACHN KO	50

Table 7: qRT-PCR RT Conditions

Step	Time	Temperature
Incubation	10 min	25°C
Reverse Transcription	2 hr	37°C

Table 7: qRT-PCR RT Conditions, Continued

Inactivation	5 sec	85°C
Hold	∞	16°C

Table 8: qRT-PCR cDNA Concentration

	cDNA Concentration (ng/μl)
HEK-293T	19.1
A-498	20.0
ACHN	16.8
HEK-293T KO	23.6
A-498 KO	39.6
ACHN KO	23.6

Table 9: qRT-PCR Cycling Conditions

Step	Time	Temperature
Initial Denaturation	2 min	94°C
40 Cycles:		
Denaturation	15 sec	94°C
Annealing, Extension and Read Fluorescence	1 min	60°C

Table 10: qRT-PCR Results

Detector	Sample	Average Cycle Threshold (Ct)	Fold Change
GAPDH	HEK	WT	13.298234
		KO	13.322624
	A-498	WT	12.178639
		KO	11.746116
	ACHN	WT	11.868929
		KO	12.062962
SMARCD1	HEK	WT	19.961655
		KO	21.672528
	A-498	WT	20.335726
		KO	20.474973
	ACHN	WT	20.429584
		KO	21.223508

Discussion

SMARCAD1 as a strong negative correlator for histone 3 citrulline protein expression

SMARCAD1 protein expression negative correlated tightly with the protein level of histone 3 citrullination both in mouse ES cells and human kidney cancer and non-cancerous cells. All cells with lower SMARCAD1 protein level exhibited comparably high protein level of histone 3 citrulline. KD and KO of SMARCAD1 gene using both siRNA and CRISPR/Cas9 techniques in both mouse and human cell lines all affected the expression of histone 3 citrulline dramatically. PADI4 protein level was altered by SMARCAD1 protein level in some of the tested cell lines through a negative feedback loop; while the final target of this feedback loop was always histone 3 citrulline. No other gene was affected by modifying SMARCAD1 level.

Though one of the antibody H3R26Cit that targeted citrulline R26 was only available for testing in the mouse cell lines, the resulting negative correlation between SMARCAD1 and this citrulline target was even stronger than antibody H3R2/8/17Cit that was later used throughout the entire study. Thus, it was anticipated to see the same hypothesis holds true for all histone 3 citrullination targets, and SMARCAD1 acts as a global negative correlator for histone 3 citrulline protein expression.

SMARCAD1 as a potential indicator of kidney cancer progression

Low to no expression of SMARCAD1 antibody staining in the majority of the renal cancer tissues [9] holds true in this study. In all three tested kidney cancer

cell lines, although the specific tumor types and patients' genders were not the same, all cell lines expressed low level of SMARCA1 protein comparing to non-cancerous kidney cells. This low and missing SMARCA1 protein level can potentially be used as an indication of the kidney cancer tumorous formation. Also, because of the negative correlation between SMARCA1 and histone 3 citrullination, the literature source has scientific explanation. Increased level of citrullination is presented in the progression of cancer [7], and based on the present study, this correlation between citrullination and cancer progression could potentially show that decreased level of SMARCA1 might be presented in the progression of cancer.

The stages of the kidney cancer cells were unable to be obtained in this study. It is possible to study the protein expression level of SMARCA1 in different stages of kidney cancer to get a sense of how SMARCA1 protein level changes with different tumor and cell stages, and if this change in expression level is a gradual process or a sudden event. This will be beneficial in determine the stages of kidney cancer progression and SMARCA1 can be a potential target for cancer treatment.

Negative correlation versus positive correlation between PADI4 and histone 3 citrullination

Negative correlation between PADI4 and histone 3 citrullination was observed in some of the cell lines, and this held true based on the positive feedback loop between SMARCA1 and PADI4 and negative correlation between SMARCA1 and histone 3 citrullination. However based on the literature,

citrullination is actually performed by enzymes PADIs [4], which suggests a positive correlation between PADI4 and histone 3 citrullination. While the observed pattern between PADI4 and citrulline protein expression can still be explained. Due to the binding of SMARCAD1 onto the Histone3 citrullination site (negative correlation), it may be difficult for PADI4 to directly catalyze citrulline formation without bypassing SMARCAD1. Potentially, there exists two distinct pathways; one is that suggested by the literature and the other is between the positive feedback loop and histone 3 citrullination. Here, SMARCAD1 acts as a pathway block and slows down the process of PADI4 catalyzed citrullination. If there is a great amount of SMARCAD1, even PADI4 has very high level of protein expression, citrullination may not occur due to the pathway blocking from SMARCAD1. On the other hand, low PADI4 protein expression can still lead to strong expression level of histone citrulline protein if there is low level of SMARCAD1 that is not sufficient to block the catalysis pathway as stated in the literature.

Conclusion

SMARCAD1 is emerging as a critical regulator of chromatin and histone modification, including protein citrullination. Together they play a crucial role in gene expression and cancer pathogenesis. The correlated protein expression between SMARCAD1, PADI4 and histone 3 citrullination observed in this study gives a better understanding of how these key players in regulating chromatin and histone are connected with one another. With respect to cancer, especially kidney cancer, the low expression of SMARCAD1 and its negative correlation with histone 3 citrullination can function as a novel cancer biomarker. Furthermore, the potential positive feedback loop between SMARCAD1 and PADI4 provides an explanation of the upstream mechanism that induces histone 3 citrulline expression. Still, due to the complexity and unpredictability of cancer cells, future analysis need to be carried out to understand the upstream mechanisms that cause the unique expression of SMARCAD1 in cancer cells.

References

- [1]. Chaker N. Adra, José-Luiz Donato, Rachel Badovinac, Farzand Syed, Reshma Kheraj, Hongbo Cai, Colin Moran, Mitchell T. Kolker, Helen Turner, Stanislaw Weremowicz, Taro Shirakawa, Cynthia C. Morton, Lowell E. Schnipper, Reed Drews, "SMARCAD1, a Novel Human Helicase Family-Defining Member Associated with Genetic Instability: Cloning, Expression, and Mapping to 4q22–q23, a Band Rich in Breakpoints and Deletion Mutants Involved in Several Human Diseases," *Genomics*, vol.69, no.2, pp.162-173, 2000.
- [2] Samuel P. Rowbotham, Leila Barki, Ana Neves-Costa, Fatima Santos, Wendy Dean, Nicola Hawkes, Parul Choudhary, W. Ryan Will, Judith Webster, David Oxley, Catherine M. Green, Patrick Varga-Weisz, Jacqueline E. Mermoud, "Maintenance of Silent Chromatin through Replication Requires SWI/SNF-like Chromatin Remodeler SMARCAD1," *Molecular Cell*, vol.42, no.3, pp.285-296, 2011.
- [3] Dawn M. Carone, Jeanne B. Lawrence, "Heterochromatin instability in cancer: From the Barr body to satellites and the nuclear periphery," *Seminars in Cancer Biology*, vol.23, no.2, pp.99-108, 2013.
- [4] Jiang Z, Cui Y, Wang L, Zhao Y, Yan S, Chang X, "Investigating citrullinated proteins in tumour cell lines," *World Journal of Surgical Oncology*, vol.11, pp.260, 2013.
- [5] Bence György, Erzsébet Tóth, Edit Tarcsa, András Falus, Edit I. Buzás, "Citrullination: A posttranslational modification in health and disease," *The International Journal of Biochemistry & Cell Biology*, vol.38, no.10, pp.1662-1677, 2006.
- [6] Cherrington BD, Morency E, Struble AM, Coonrod SA, Wakshlag JJ, "Potential Role for Peptidylarginine Deiminase 2 (PAD2) in Citrullination of Canine Mammary Epithelial Cell Histones," *PLoS ONE*, 2010.
- [7] Van Venrooij WJ, Pruijn GJM, "Citrullination: a small change for a protein with great consequences for rheumatoid arthritis," *Arthritis Research*, vol.2, no.4, pp.249-251, 2000.
- [8] Zhang X, Bolt M, Guertin MJ, Chen W, Zhang S, Cherrington BD, Slade DJ, Dreyton CJ, Subramanian V, Bicker KL, Thompson PR, Mancini MA, Lis JT, Coonrod SA, "Peptidylarginine deiminase 2-catalyzed histone H3 arginine 26 citrullination facilitates estrogen receptor α target gene activation," *Proceedings of the National Academy of Sciences of the United States of America*, vol.109, no.33, pp.13331-13336, 2012.
- [9] "SMARCAD1," *The Human Protein Atlas*, 16 May 2016.

[10] Slade DJ, Subramanian V, Thompson PR, "Citrullination Unravels Stem Cells," *Nature chemical biology*, vol.10,no.5,pp.327-328,2014.

[11] Mali P, Yang L, Esvelt KM, Aach J, Guell M, DiCarlo JE, Norville JE, Church GM, "RNA-Guided Human Genome Engineering via Cas9," *Science*, vol.339,pp.823-826,2013.

[12] Cong L, Zhang F, "Genome Engineering Using the CRISPR-Cas9 System." *Methods in Molecular Biology*, pp.197-217,2015.